Building and Environment 223 (2022) 109397

Contents lists available at ScienceDirect

Building and Environment

journal homepage: www.elsevier.com/locate/buildenv

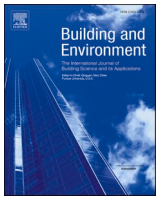

Impact of climate change on nearly zero-energy dwelling in temperate climate: Time-integrated discomfort, HVAC energy performance, and GHG emissions

Ramin Rahif [a,*], Alireza Norouziasas [a], Essam Elnagar [b], Sébastien Doutreloup [c], Seyed Mohsen Pourkiaei [d], Deepak Amaripadath [a], Anne-Claude Romain [d], Xavier Fettweis [c], Shady Attia [a]

[a] Sustainable Building Design Lab, Dept. UEE, Faculty of Applied Sciences, University of Liège, Belgium
[b] Thermodynamics Laboratory, Aerospace and Mechanical Engineering Department, Faculty of Applied Sciences, Université de Liège, 4000, Liège, Belgium
[c] Laboratory of Climatology and Topoclimatology, Department of Geography, UR SPHERES, University of Liège, Belgium
[d] University of Liège, Faculty of Sciences, Department of Environmental Science and Management, Sensing of Atmospheres and Monitoring (SAM), Avenue de Longwy 185, 6700, Arlon, Belgium

ARTICLE INFO

Keywords:
Global warming
Heating energy use
Cooling energy use
Primary energy use
Overheating
Overcooling

ABSTRACT

Global warming is widely recognized to affect the built environment in several ways. This paper projects the current and future climate scenarios on a nearly zero-energy dwelling in Brussels. Initially, a time-integrated discomfort assessment is carried out for the base case without any active cooling system. It is found that overheating risk will increase up to 528%, whereas the overcooling risk will decrease up to 32% by the end of the century. It is also resulted that the overheating risk will overlap the overcooling risk by 2090s under high emission scenarios. Subsequently, two commonly applied HVAC strategies are considered, including a gas-fired boiler + an air conditioner (S01) and a reversible air-to-water heat pump (S02). In general, S02 shows ~6–13% and 15–27% less HVAC primary energy use and GHG emissions compared to S01, respectively. By conducting the sensitivity analysis, it is found that the choice of the HVAC strategy, heating set-point, and cooling set-point are among the most influential parameters determining the HVAC primary energy use. Finally, some future recommendations are provided for practice and future research.

1. Introduction

Climate change arising from natural or anthropogenic sources causes long-term shifts in temperatures and weather patterns. According to Intergovernmental Panel on Climate Change (IPCC) Sixth Assessment Report (AR6), the average global surface temperature is expected to increase in the range of 1–5.7°*C* depending on the Shared Socioeconomic Pathway (SSP) scenario [1]. In addition, the Urban Heat Island (UHI) effect is recognized in more than 400 cities around the world [2,3]. The UHI effect, defined as *"relatively atmospheric warmth of urban areas compared to the surrounding countryside",* is predicted to increase the ambient temperature in cities by 5–10°*C* [4,5]. It is necessary to project such warming weather conditions on buildings to predict the changes in comfort conditions as well as Heating Ventilation, and Air Conditioning (HVAC) energy use and Green House Gas (GHG) emissions.

The impact of climate change on thermal comfort in different locations will vary depending on the climate. In temperate climates, a major anticipated impact of climate change is the increase of overheating occurrence and associated health hazards for the occupants in buildings [6–10]. Overheating affects the occupants' comfort [11], productivity [12] and health, where in severe cases can lead to illness and death [13,14]. In total, over 35,000 people died in Europe during the summer 2003 heatwave [15], in which 14,729 deaths are reported in France [16], 2139 in England and Wales [17], up to 2200 in the Netherlands [18], and 1175 in Belgium [19]. Therefore, there is a need to evaluate the future thermal performance of the buildings and equip them, if necessary, with sustainable and resilient cooling solutions to ensure the comfort and well-being of the occupants.

Several methods are introduced in the scientific literature to evaluate

* Corresponding author.
E-mail address: ramin.rahif@uliege.be (R. Rahif).

https://doi.org/10.1016/j.buildenv.2022.109397
Received 28 February 2022; Received in revised form 7 July 2022; Accepted 11 July 2022
Available online 1 August 2022

thermal comfort, described as *"the condition of mind that expresses satisfaction with the thermal environment and is assessed by subjective evaluation"* [20]. Recently, a new group of methods have been proposed (which are the focus of the current study) to assess the thermal comfort over a span of time in buildings that are named as *time-integrated, long-term, or chronic comfort evaluation methods* [20–23]. In other words, they quantify the accumulation of discomfort stimuli over a specific period. Most of those methods are aimed at assessing the overheating discomfort (asymmetric), whereas some deal with both overheating and overcooling discomfort (symmetric), and only a few of them developed for overcooling discomfort [24,25]. Previous studies reviewed such methods highlighting their strengths and limitations [21,25–27].

According to European Commission (EC), the buildings in the EU account for 40% of energy consumption and 36% of Green House Gas (GHG) emissions [28]. Heating and cooling make for the majority of building energy use in Europe, accounting for 70% of total energy consumption in residential units [29]. This highlights the potential of buildings, in particular HVAC systems, in reducing energy consumption and GHG emissions [30]. Climate change influences the HVAC size and energy demand [31]. With the continuation of global warming, energy demand for heating and cooling is predicted to decrease and increase, respectively [32]. However, the rate of change in different locations will vary depending on the climate [33]. Consequently, the future climatic forecasts must be included in the building energy simulations to better understand the trend of energy consumption and GHG emissions for the HVAC components as the major energy consumers in the buildings.

Table 1 lists some studies that discussed the impact of climate change on time-integrated discomfort, heating demand, cooling demand, and GHG emissions in residential buildings in Europe. Sajjadian et al. [34] evaluated a four-story flat in compliance with the Passive House standard in London. By applying future weather data obtained from morphing the UK Climate Impact Program (UKCIP) monthly climate data using CCWorldWeatherGen tool, a significant shift towards less overcooling was resulted from 2011 to 2080. It was also found that the overall energy consumption decreases because of considerably higher reduction in the heating demand compared to the increase in the cooling demand. Attia S. and Gobin C [35]. evaluated a nearly Zero-Energy Building (nZEB) located in Eupen municipality in Belgium using the future weather data downscaled by the regional climate model (MAR) "Modèle Atmosphérique Régional". The outcomes of the study showed that the passive design strategies could not prevent overheating in naturally ventilated and highly insulated case study. Considering EN15251 adaptive comfort model, the overheating hours rises 700 h, 845 h, and 1441 h by 2100 for the RCP4.5, RCP6, and RCP8 scenarios, respectively. They also suggested that the active cooling strategies may become the most practical option if the overheating hazards are not addressed during the building design. Ciancio V. et al. [36] studied the impact of climate change on energy demands in 19 European cities covering the main Köppen-Geiger climate classes (B - arid; C – temperate; D - continental; E – polar). A representative case study consisting of three floors and three apartments was considered for all cities. The weather data are obtained from real observations (current: 2020) and CCWorldWeatherGen tool (future: 2050 and 2080). It was found that in cities such as Copenhagen, Gothenburg and Paris the CO_2 emissions tend to decrease, whereas in some other cities such as Milan, Porto, and Berlin, the CO_2 emissions tend to increase. Taken together all the examined cities, they found that the increase in cooling demands will offset the decrease in heating demands; therefore, the energy consumption and CO_2 emissions will rise globally. It was also found that in cities such as Copenhagen, Gothenburg, London, and Prague, it will become necessary to install active cooling systems (if not present) to ensure comfort conditions in the future. In addition to the above-mentioned studies, other similar studies can be found at building scale [36–48] and building stock scale [49–51] in the scientific literature (see Table 1).

Despite the numerous studies on climate change impact assessment in buildings, there is relatively less comprehensive research including all aspects of time-integrated discomfort, HVAC primary energy use, and GHG emissions. They mostly lack a multizonal and asymmetric assessment of time-integrated discomfort [21] with high-resolution climate

Table 1
Summary of the recent studies on the impact of climate change on Time-integrated Discomfort (TiD), Heating Demand (HD), Cooling Demand (CD), and GHG Emissions (GE) in residential buildings in Europe.

Author(s)	Ref.	Year	Building type (study scale)	Location	Focus
Frank Th.	[41]	2005	Multistory residential unit (building scale)	Zurich–Kloten, Switzerland	HD, CD
Olonscheck M. et al.	[51]	2011	Residential buildings (building stock scale)	Germany	HD, CD, GE
Nik V. and Kalagasidis AS.	[50]	2013	Residential buildings (building stock scale)	Stockholm, Sweden	HD, CD
Jylhä K. et al.	[52]	2015	Detached residential house (building scale)	Southern Finland	HD, CD
Van Hooff T. et at.	[45]	2016	Terraced dwelling (building scale)	De Bilt, Netherlands	HD, CD
Sabunas A. and Kanapickas A.	[38]	2017	Four-story residential unit (building scale)	Kaunas, Lithuania	HD, CD
Sajjadian SM.	[34]	2017	Four-story residential unit (building scale)	London, UK	TiD, HD, CD
Tettey U. et al.	[39]	2017	Multi-story residential unit (building scale)	Växjö, Sweden	HD, CD
Andrić I. et al.	[43]	2017	Six-story detached residential unit (building scale)	6 cities including Madrid, Spain & Milan, Italy, & Hamburg, Germany	HD
Pérez-Andreu V. et al.	[47]	2018	Single-family detached house (building scale)	Valencia, Spain	TiD, HD, CD
Ciancio V. et al.	[44]	2019	Three-story residential unit (building scale)	Aberdeen, Scotland & Prague, Czech & Palermo, Italy	HD, CD
Moazami A. et al.	[46]	2019	16 building types including high- and mid-rise residential units (building scale)	Geneva, Switzerland	HD, CD
Attia S. and Gobin C.	[35]	2020	Three-story single-family detached house (building scale)	Eupen, Belgium	TiD
Ciancio V. et al.	[36]	2020	Three-story representative apartment (building scale)	19 European cities	HD, CD, GE
Machard A. et al.	[37]	2020	Single-story residential unit (building scale)	Paris, France	HD, CD
Shen J. et al.	[40]	2020	A flat in multi-family apartment (building scale)	Rome, Italy & Stockholm, Sweden	TiD
De Masi R. F. et al.	[48]	2021	Single-family representative house (building scale)	Benevento, Italy	HD, CD
Yang Y. et al.	[49]	2021	Residential buildings (building stock scale)	38 European cities	TiD, HD, CD
Pajek L. et al.	[42]	2022	Single-family detached unit (building scale)	Moscow, Russia & Ljubljana, Slovenia & Milan, Italy & Athens, Greece & Porto, Portugal	HD, CD

data [53]. In addition, most studies are carried out by a unique assumption on the type of the HVAC system without detailed information on their modelling procedure. The above is more evident in the studies performed in temperate climates in Europe. Therefore, as members of the International Energy Agency (IEA) EBC Annex 80 – "Resilient cooling of buildings" project, we developed this paper to address the abovementioned knowledge gap inspired by the framework developed within the project [8]. The aim of this research is to extend the knowledge on thermal comfort and energy performance of residential buildings in the context of climate change and broaden the comparative analysis among HVAC strategies to come up with the most sustainable solutions. The research questions are:

- Q1: What will be the changes in outdoor weather conditions assuming different emission scenarios for Brussels?
- Q2: To what extent climate change will affect time-integrated discomfort in a naturally ventilated nearly zero-energy dwelling?
- Q3: What will be the changes in HVAC primary energy use and GHG emissions under the operation of commonly applied HVAC systems?
- Q4: What are the influential parameters (i.e., weather data, the choice of the HVAC system, the HVAC performance characteristic, and set-point temperatures) in determining the HVAC primary energy use?

This paper provides a valuable contribution to the new body of knowledge from an international perspective by providing a clear picture of climate change impact assessment in temperate oceanic climates (Cfb) according to Köppen-Geiger-Peel climate classification [54]. Such climate is particularly dominant in Western Europe in cities like Amsterdam, Brussels, Copenhagen, London, and Paris. As can be seen in Fig. 1, in addition to European cities, some major cities such as Auckland, Bogotá, Canberra, Nairobi, Vancouver, and Santa Fe have a similar climate in other regions around the world. This paper also applies a multizonal method in quantification of time-integrated discomfort in buildings. More importantly, a new fit-to-purpose metric called "*Indoor overcooling Degree (IOcD)*" is proposed to provide a full asymmetric assessment together with a previously developed metric called "*Indoor Overheating Degree (IOhD)*" [10]. This paper also compares two HVAC strategies, including a gas-fired boiler for heating + Air Conditioner (AC) for cooling and a reversible air-to-water heat pump for both heating and cooling. Both strategies include mechanical ventilation with a heat recovery system. The detailed information on their sizing is provided while incorporating the uncertainties in the input parameters (uncertainty analysis). Last but not least, this paper includes sensitivity analysis (SA) to identify the most influential factors affecting the HVAC primary energy use.

For policymakers, this paper sheds light on the importance of climate change-sensitive comfort evaluations and criteria to be embedded in the building codes. This can result in comfort benefits and helps the construction sector towards climate change proof residential buildings. This paper also informs the building professionals about the future of HVAC related energy use and GHG emissions and how their choice of the HVAC system can affect them. The current paper is organized as follows. In Section 2, the methodology is provided, including the boundary conditions (Section 2.1), climate data (Section 2.2), building model (Section 2.3), time-integrated discomfort evaluation (Section 2.4), and HVAC strategies (Section 2.5). Section 3 presents the results. Section 4 discusses the key findings, recommendations, strengths, limitations, and implications on the practice of the study and suggests potential future research. And, Section 5 concludes the paper.

2. Methodology

Fig. 2 shows an overview of the current paper's methodology. In the first stage, the base case building model is created and simulated to analyze the indoor thermal conditions in different weather scenarios. In the second stage, two different designs for the HVAC system (i.e., S01 and S02) are considered. DesignBuilder v7.0.0 software is used to create the building and HVAC models, which is a comprehensive and intuitive Graphical User Interface (GUI) for the EnergyPlus simulation engine. In the second stage, the exported Input Data File (.idf) from DesignBuilder is fed into JEPlus and JEPlus + EA open-source software to perform the uncertainty and sensitivity analysis, respectively. JEPlus is a tool to manage complex parametric analysis based on the EnergyPlus simulation engine, while JEPlus + EA is an extension for JEPlus to conduct full-factorial, Monte Carlo, global sensitivity, and constrained multi-objective optimization [55]. In total, over 16000 simulations are run in 72 h using a workstation with CPU: AMD 3990X - 64 × 2.9 GHz, Cache: 256 MB, RAM: 64 GB, and Graphics card: 24 GB (2 × 32 GB). The post-processing and visualizations are done using a homemade MATLAB script.

2.1. Boundary conditions

In this section, the boundary conditions assumed for the current study are presented. First, the study is performed on a representative case in Belgium characterized by temperate climate. In such heating-dominated regions, the focus of building design is mainly on heat preservation during the winter season. This is achieved via highly insulated and airtight design concepts hindering heat dissipation during

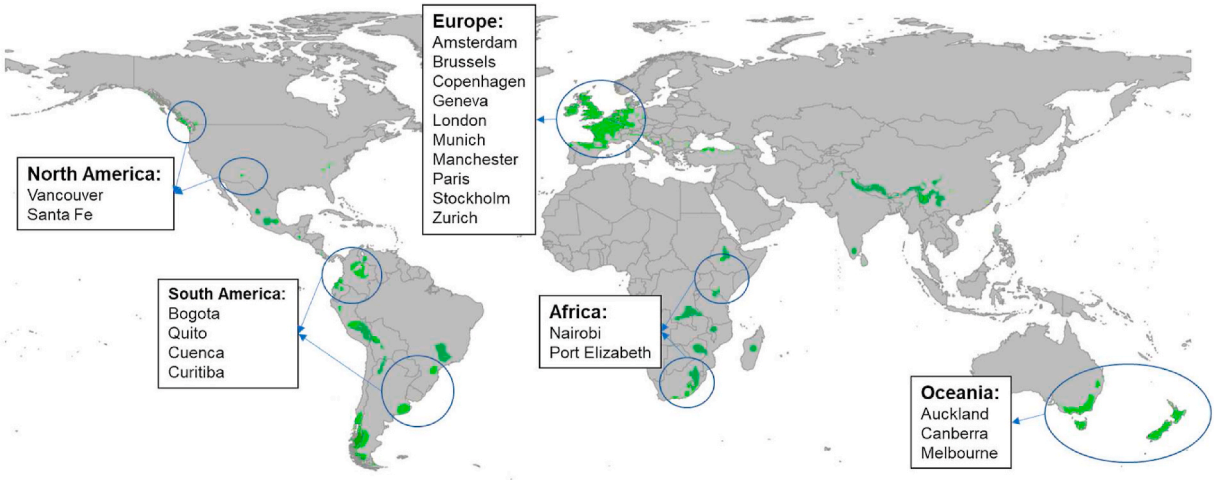

Fig. 1. Cities with temperate oceanic climate (Cfb) worldwide [54].

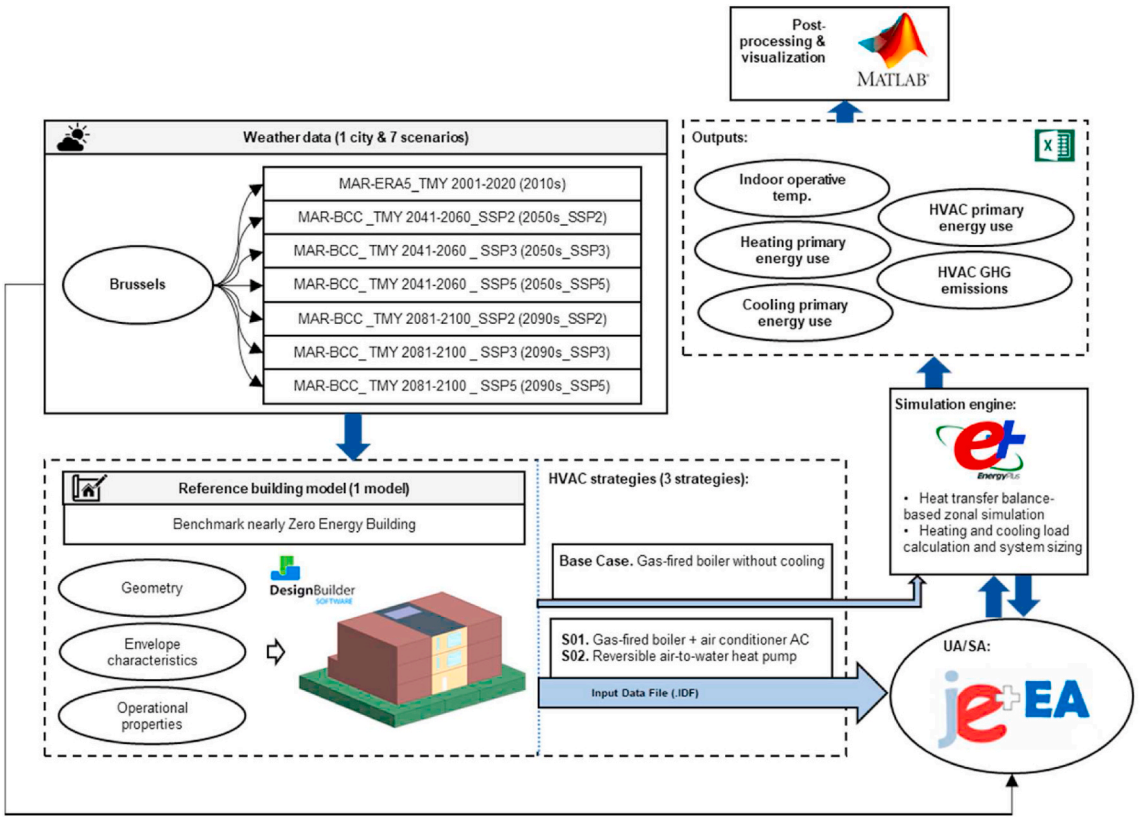

Fig. 2. Study conceptual framework (SCF).

the summer season. Therefore, by only relying on passive measures, it may become difficult in the future to prevent overheating issues. It should be mentioned that the provisions are required (e.g., reference building model, climate data, GHG emissions intensity, etc.) to the generalizability of the results to other temperate regions.

Second, the study's focus is restricted to the comparison of two commonly applied HVAC strategies. As the first HVAC strategy, an air conditioner is added to provide cooling along with the existing gas-fired boiler for heating. It is a cost-effective measure because there is no need for ductwork, and it requires minor changes to the building for fitting the components. As the second HVAC strategy, a reversible air-to-water heat pump is implemented that provides heating, cooling, and consistent Domestic Hot Water (DHW). Unlike air-to-air heat pumps, air-to-water heat pumps do not require additional systems to provide DHW. The air-to-water heat pumps are suitable for households for replacing the traditional boilers with a more environmentally friendly option with a relatively high installation cost. Other boundary conditions of the current study are that a) there is no consideration regarding degradation of building envelope and the HVAC components and b) there is no consideration regarding the evolution of GHG emissions factor based on the energy mix of the electricity production.

2.2. Climate data

Acquiring reliable current and future climate data is vital in any study related to climate change and defines its quality [47]. In this paper, the climate data are based on the General Circulation Model (GCM) outputs. The GCMs are used to estimate the climate projections, whereas they are not directly applicable to building simulations due to high spatial and temporal resolutions. It is necessary to transform them into compatible climate data using downscaling techniques (statistical or dynamical methods). For this aim, the regional climate model (MAR) *"Modèle Atmosphérique Régional"* was used in its version 3.11.14 [56], which is a dynamical method resulting in physically consistent climate parameters and extreme weather events. MAR is adapted and widely validated for Belgium region [57–59].

MAR is derived by coupling a three-dimensional atmospheric model to a one-dimensional transfer scheme between the atmosphere, vegetation, and surface [60]. To calculate the climate data used in this paper, two different methods were implemented. First, MAR was forced every 6 h in its lateral boundaries by reanalysis ERA5 [61] assimilated by different sources of observations (e.g., in-situ weather station, radar data, satellites, etc.) between 1980 and 2014. This can be considered as the reconstruction of observed climate data. Second, MAR was forced every 6 h by Earth System Model (ESM) BCC-CSM2-MR (which approximately follow the mean temperature of all ESMs over Belgium up to 2100) from the Sixth Coupled Model Intercomparison Project (CMIP6) that represents the mean evolution of climate parameters between 1980 and 2014 with the historical scenario and 2015–2100 with the SSPs [62]. ESM forced MAR was then validated by comparing to MAR ERA5 simulations to verify whether it can be used to generate future climate data [56].

ESMs for future periods are based on Shared Socioeconomic Pathways (SSPs). SSPs are projected scenarios of global socioeconomic evolution by 2100. SSPs are used to quantify Green House Gas (GHG) emissions associated with different climate policies. The future climate data in this paper consists of three SSPs, 1) SSP2 – medium challenges to mitigation and adaptation ($1.8°C$ estimated global warming by 2100), 2) SSP3 – high challenges to mitigation and adaptation ($3.6°C$ estimated global warming by 2100), and 3) SSP5 – high challenges to mitigation and low challenges to adaptation ($4.4°C$ estimated global warming by 2100) [63,64].

After obtaining the results of MAR forced by BCC-CSM2-MR, the Typical Meteorological Years (TMYs) are constructed over 20 years for three different periods 2001–2020 (hereafter 2010s), 2041–2060 (hereafter 2050s), and 2081–2100 (hereafter 2090s). TMYs are

synthetic years (on an hourly basis) formed by typical representative months selected from the target period (e.g., 2001–2020) (i.e., January from 2001, February from 2012, etc.). The typical months are chosen by comparing the distribution of each month in the long-term distribution of that month for the available modelled or observed data (minimum 10 years) using Finkelstein-Shafer statistics. The protocol by ISO 15927–4 [23] was used to create the TMYs. The weather data in this paper are derived for Brussels (Köppen–Geiger climate zone: Cfb, Marine west coast and warm summer) from Ref. [56]. The selection of the periods and emission scenarios (SSPs) for the weather files in this paper are inspired by the recommendations of the dynamic simulation guideline developed within International Energy Agency (IEA) EBC Annex 80 – "Resilient cooling of buildings" project [65] as well as a previous study in the literature [8].

2.3. Building model

A reference building model representing a typical terraced dwelling in Belgium is adopted for this study based on the work of [66]. The building is located in Brussels (50°83′79″, 4°44′10″, 13 m) and was renovated after 2010 to comply with the nearly Zero-Energy Building (nZEB) requirements. The envelope is externally insulated, and photovoltaic panels are mounted on the roof. The building was constructed in three floors and has north- and south-facing glazing areas. The reference building is presented in Fig. 3.

The datasets regarding the building model in.dsb (DesignBuilder model data) and.idf (EnergyPlus input data file) formats are extracted from Ref. [67]. The multizonal building model includes the conditioned zones categorized as, 1) living areas (living room and open kitchen as one zone), 2) office room, 3) three bedrooms, and 4) five short-presence areas (two corridors, two bathrooms, one WC).

The building is occupied by a family of two parents (above 45 years old) and two children (seven and ten years old). The occupancy schedules are specified based on ISO 18253–2 [68] with a density of 43 m^2/person. ISO 18253–2 provides occupancy schedules for a four-member family with 46 years old householders. According to Ref. [66], the same occupancy schedules are defined for weekdays and weekends. Based on the data collected in the surveys, the lighting power intensity of 10 W/m^2 is assigned for the living areas, while the lighting power intensity of 8 W/m^2 is assigned for the bedrooms. The lighting schedules are tuned for the winter season and validated by using the outcomes of national energy reports provided by the Flemish Energy Agency (FEA) and IP Belgium. Table A1 in Annex A summarizes the characteristics of the calibrated building model.

In the base case building model, the heating is provided by a gas-fired boiler with a hydronic loop coupled to the radiators and there is no active cooling. The temperature set-points for heating are set to 21°*C* in living areas, 18°*C* in bedrooms, and 18°*C* in short-presence areas. The building is naturally ventilated during the occupied hours in the summer with control on minimum indoor air temperature of 24°*C*. Mechanical ventilation with a heat recovery system is also operating to provide minimum fresh air of 25 m^3/h according to NBN D50-001. In addition, the Photovoltaic (PV) panels are attached to the roof adjacent to the northern edge. The PV panels have Crystalline Silicon cell type (36 cells in series) with an active area of 0.34 m^2 and rated electric power output of 61 Watt. The PV panels are connected to a DC to AC converter with an efficiency of 0.95. According to Ref. [66], the on-site electricity generation of PV panels is 3000 kWh/year.

2.4. Time-integrated discomfort evaluation

The time-integrated discomfort evaluation in buildings requires the determination of indicators and underlying thermal comfort models (if required). The time-integrated discomfort indicators can be symmetric (overheating- and overcooling-specific) or asymmetric (overheating-specific or overcooling-specific) [21]. Following the recommendations of the guidelines developed in International Energy Agency (IEA) EBC Annex 80 – "Resilient cooling of buildings" project [65,69] and the scientific literature [8,21], an asymmetric index called Indoor Overheating Degree (IOhD) [10] is selected to estimate the overheating discomfort. Afterwards, a new asymmetric index is proposed in this study named as Indoor Overcooling Degree (IOcD) to quantify the overcooling discomfort separately. The *IOhD* and *IOcD* indices accumulate heating and cooling degree hours over the total number of zonal occupied hours, respectively. The formulas to calculate the *IOhD* and *IOcD* are,

$$\mathrm{IOhD} \equiv \frac{\sum_{z=1}^{Z}\sum_{i=1}^{N_{occ}(z)}\left[\left(T_{in,z,i}-T_{comf,upper,z,i}\right)^{+}\times t_{i,z}\right]}{\sum_{z=1}^{Z}\sum_{i=1}^{N_{occ}(z)} t_{i,z}} \tag{1}$$

$$\mathrm{IOcD} \equiv \frac{\sum_{z=1}^{Z}\sum_{i=1}^{N_{occ}(z)}\left[\left(T_{comf,lower,z,i}-T_{in,z,i}\right)^{+}\times t_{i,z}\right]}{\sum_{z=1}^{Z}\sum_{i=1}^{N_{occ}(z)} t_{i,z}} \tag{2}$$

Where Z [−] is the number of total building conditioned zones, $N_{occ}(z)$ [−] is the total number of occupied hours in zone z, $T_{in,o,z}$ is the indoor operative temperature in zone z at hour i, $T_{comf,\mathrm{upper},z,i}$ is maximum comfort threshold in zone z at hour i, $T_{comf,\mathrm{lower},z,i}$ is minimum comfort threshold in zone z at hour i. The $T_{comf,\mathrm{lower},z,i}$ and $T_{comf,\mathrm{upper},z,i}$ can be derived from the static or adaptive comfort models in the standards such as ISO 17772, EN 16798, ASHRAE 55, CIBSE Guide A, etc.

The *IOhD* and *IOcD* are multizonal indices that quantify, with a single

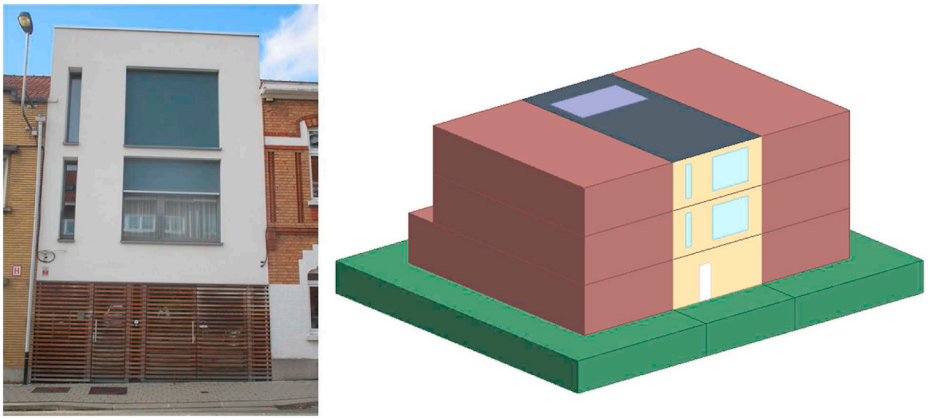

Fig. 3. The representative nearly zero-energy terraced dwelling in Belgium.

value, the intensity and frequency of discomfort in a building. Such a multizonal approach allows depicting real-world circumstances in buildings, encompassing zones with variable thermal comfort models (i.e., static and adaptive) and requirements (e.g., comfort categories), as well as tracking the occupied hours in each zone. This makes it easier to reflect the zone-based occupant behavior and adaptation opportunities. Therefore, the time-integrated discomfort assessment via those metrics is adaptable and allows for personalization at the zone level under real and artificial conditions.

In this paper, the comfort models are obtained from ISO 17772-1 standard. ISO 17772–1 provides category-based static (Cat. I, Cat. II, Cat. II and Cat. IV) and adaptive (Cat. I, Cat. II, and Cat. III) comfort models. Category II is selected in this study that is recommended for new buildings and renovations [21,25]. For the bedrooms, the static comfort model is chosen due to the limited occupant adaptation actions during the sleeping period [70]. The static comfort model in ISO 17772–1 is provided in PMV/PPD ranges that can be translated into the operative temperature ranges by setting assumptions on relative humidity (=40% for the heating season and = 60% for the cooling season), air velocity (<0.1 m/s), metabolic rate (~1.2 met), and clothing factor (~0.5 clo for summer and ~1 clo for winter). Consequently, $20°C$ and $26°C$ are assigned for the bedrooms as the lower limit and upper limit of comfort, respectively. For other zones, the adaptive comfort model is selected that is recommended for naturally ventilated buildings. The adaptive comfort model in ISO 17772–1 is provided via the formulas for the upper and lower limit of comfort based on the weighted running mean outdoor air temperature T_{rmo} [71]. The formulas to calculate the upper and lower limits in Category II are,

$$T_{comf,upper,z,i} = 0.33T_{rmo} + 18.8 + 3 \quad (3)$$

$$T_{comf,lower,z,i} = 0.33T_{rmo} + 18.8 - 4 \quad (4)$$

2.5. HVAC strategies

2.5.1. Gas-fired boiler (heating) + air conditioner (cooling)

As the first HVAC strategy (S01), a split Air Conditioner (AC) is added to the base case to provide cooling without changing the existing gas-fired boiler system (see Section 2.3). A gas-fired boiler connects to flow splitters and mixers together with a circulating pump to provide hot water for heating and domestic use. A conventional split AC, as implied by its name, consists of an indoor and an outdoor unit. The outdoor unit includes an air-cooled condenser, a condenser fan, and a compressor, while the indoor unit includes an evaporator, an expansion valve, and a distribution fan. The AC circulates the indoor air and cools it before the supply node by passing it over the evaporator coil. The AC cooling capacity is controlled by varying the indoor unit fan speed or AC/DC compressor inverter. The AC deals with both sensible and latent heat loads.

The gas-fired boiler is modelled in DesignBuilder using Hot Water Plant Loop module. It requires the boiler definition in terms of fuel type, rated heating capacity, rated thermal efficiency, and design flow rates. The amount of fuel used in the boiler is calculated by the combination of rated thermal efficiency and normalized efficiency performance curve. The performance curve is set to the default curve as CondensingBoilerEff and shows the fraction of nominal thermal efficiency of the boiler based on the hot water temperature leaving the boiler.

The AC in DesignBuilder can be implemented by using a unitary single zone module. The unitary single zone module allows modelling a constant volume direct-expansion cooling via the DX cooling coil. The DX cooling coil uses the combination of the rated Sensible Heat Ratio (SHR), rated total cooling capacity, rated air volume flow rate, and rated *EER*. It also requires the definition of availability schedules which is considered identical to the occupancy schedules in this study. In this paper, to define the DX coil performance under a range of conditions, the default performance curves are selected from the EnergyPlus database. For instance, DXClgCoilTotalClgCap/EnergyInputRatioFuncTemperature are selected that are bi-quadratic curves representing the total cooling capacity/Energy Input Ratio (EIR) as a function of temperature curves. In other words, they show the variations in total cooling capacity/EIR as a function of the wet-bulb temperature of the inlet air passing over the cooling coil and the dry-bulb temperature of the air entering the condenser coil. The output of this curve is then multiplied by the rated cooling capacity/EIR to show the total cooling capacity/EIR at a specific temperature operating condition.

2.5.2. Reversible air-to-water heat pump (heating & cooling)

As the second HVAC strategy (S02), a reversible air-to-water heat pump is implemented to provide both heating and cooling. Similar to the AC system, the reversible air-to-water heat pump has an indoor and an outdoor unit. In the heating mode, the outdoor unit coil operates as an evaporator by extracting the heat from the outdoor air by forcing the refrigerant to transform from the liquid phase to the gas phase. The gas is then compressed in the compressor to increase its temperature. The indoor unit coil acts as a condenser and transfers the heat from the gas into the hydronic loop. The heated water is stored in a tank with a supplemental electric heater. The stored hot water can serve the DHW or can be circulated in radiators, fan coils, or radiant surfaces. This process can be easily reversed to provide the chilled water during the cooling season using a 4-way valve (the evaporator becomes condenser, and the condenser becomes evaporator).

To model a reversible heat pump in DesignBuilder, different hot- and chilled-water loops should be defined. For hot water loop, an air-to-water heat pump module is implemented that consists of an air-to-water DX compression coil as a primary source connected to a water tank with a supplemental heater as a secondary/additional source for heating. The DX coil object calculates the air-side heating capacity in parallel to the water-side temperature gradient at a given condenser flow rate. To define the performance of the DX coil in different operating conditions in terms of the *COP* and total heating capacity, ASHPLowTCAPFT (heating capacity function of evaporator wet-bulb temperature) and ASHPLowTCOPFT (heating COP function of evaporator wet-bulb temperature) bi-quadratic curves are selected from the EnergyPlus database. For the chilled water loop, a high-temperature chilled water loop is defined consisting of an air-cooled condenser, an evaporator, and a compressor to supply chilled water at $\sim 18°C$. The performance curves and the characteristics of the components for the chilled water loop are derived from the manufacturer's data.

For both S01 and S02, all thermal capacities and design flow rates are auto-sized by EnergyPlus based on the external design conditions and the building configuration. For this aim, the summer and winter design data should be specified that are simplified weather data based on the most extreme days. The auto-sizing feature uses design day weather data to specify outside conditions when auto-sizing the HVAC components based on ASHRAE sizing method [72]. The design data for cooling consists of maximum dry-bulb temperature, coincident wet-bulb temperature, and minimum dry-bulb temperature. The design data for heating consists of minimum dry-bulb temperature, wind speed, and wind direction. For each period, the degree of confidence of the design data should be selected. In other words, the probability that the design data will occur in reality should be defined. This can be done based on the dry- or wet-bulb temperatures with 99.6%, 99%, and 98% confidence (i.e., 0.4%, 1%, and 2% chance of more extreme weather occurrence). 99.6% confidence is assumed in this paper. The auto-sizing feature sizes the HVAC components in a way to fit the loads and maintain comfort for all periods except for more extreme conditions than the design data. In this paper, the design data are derived from the current weather data (i.e., 2010s) and kept the same considering a non-climate change responsive design (i.e., the HVAC components are not re-sized based on the future summer and winter design data) [8]. In both strategies, the existing mechanical ventilation with a heat recovery system is kept providing minimum fresh air of 25 m^3/h according to NBN

D50-001. Both strategies are among widely available (TRL∼9) and applicable HVAC systems in temperate climates [73]. All the input values to model S01 and S02 are listed in Table 2.

2.6. Uncertainty and sensitivity analysis method

This section provides an overview of the Uncertainty Analysis (UA) and the Sensitivity Analysis (SA) and their application in this study.

The UA is the practice of quantifying the variability of the output parameters due to the variability of the input parameters in an input/output dataset. It results in the estimation of statistical factors such as mean, median, and population quantiles of the output parameters. A sampling-based uncertainty analysis called Latin Hypercube Sampling (LHS) [74] is used in this study where a set of probability distribution of the input parameters are sampled to be propagated within the simulation model to obtain the distribution of the selected output parameters. The LHS method is extensively used due to relatively its small sample size (low computational cost) and efficient stratification properties [75]. Details for the LHS can be found in Refs. [76,77].

The SA studies to what extent the variations in the input parameters qualitatively or quantitatively vary the output parameters [78]. The SA can be divided into local SA and global SA. The latter is used in this study that characterizes the effect of the input parameters over the entire input space and helps discard the parameters with negligible effect in order to reduce the computational burden [79]. For this aim, the Morris method is used [80]. The Morris method uses a set of randomized One variable at a Time (OAT) design experiments [79] that vary only one parameter keeping the other parameters constant in each run. The main advantage of the Morris method is the low computational cost; however, it is not able to distinguish non-linear interactions between the input and output parameters [81].

Since this paper deals with modelling the HVAC systems in the future, it is necessary to account for the evolution of some key parameters characterizing their performance. Accordingly, some of those parameters are selected as input parameters for UA/SA, including the *COP* of the air-to-water heat pump (in heating mode) *"P0"*, gas-fired boiler efficiency *"P1"*, EER of the air-to-water heat pump (in cooling mode) and the AC *"P2 & P3"*, and mechanical ventilation fan efficiency *"P4"*. Due to foreseen advancements in the HVAC industry in the future, the input parameters are defined as improving ranges (i.e., the current values from the manufacturer's data are considered as the minimum value). In addition, in line with the work of [31], the set point temperatures for heating *"P5 & P6"* and cooling *"P7"* are added as the input parameters for the UA/SA. All the input parameter ranges regarding the HVAC systems are listed in Table 2. The output parameters are defined to fit the scope of the current paper including the heating primary energy use [kWh/m^2] *"t0"*, cooling primary energy use [kWh/m^2] *"t1"*, HVAC primary energy use [kWh/m^2] *"t2"*, and HVAC GHG emissions [ton] *"t3"*.

The SA is performed for S01 and S02 individually and combined (i.e., considering the building model as a discrete input parameter *"M"*). This allows exploring the most influential parameters affecting the HVAC primary energy use for each of the HVAC systems individually as well as to rank the effect of decision making regarding the type of the HVAC system on its primary energy use.

In this paper, JEPlus parametric tool is used to perform UA based on the LHS method and JEPlus + EA is used to perform SA based on the Morris method with a sample size of 600, max generations 300, and first population size of 50.

3. Results

3.1. Evolution of outdoor weather conditions

Fig. 4 shows the monthly outdoor air temperature for current and future TMYs for Brussels resulted from MAR forced by BCC-CSM2-MR

Table 2
The HVAC model inputs for S01 and S02.

	Gas-fired boiler + air conditioner (S01)	Reversible air-to-water heat Pump (S02)
Target zones (heating)	Living & kitchen, office, bedroom 01, bedroom 02, bedroom 03, corridors, WC, bathroom 01, and bathroom 02	Living & kitchen, office, bedroom 01, bedroom 02, bedroom 03, corridors, WC, bathroom 01, and bathroom 02
Target zones (cooling)	Living & kitchen, office, bedroom 01, bedroom 02, and bedroom 03	Living & kitchen, office, bedroom 01, bedroom 02, and bedroom 03
Target zones (ventilation)	Living & kitchen, office, bedroom 01, bedroom 02, bedroom 03, WC, bathroom 01, and bathroom 02	Living & kitchen, office, bedroom 01, bedroom 02, bedroom 03, WC, bathroom 01, and bathroom 02
Set-point temperatures [°C]	[Min: 20°C, Int: 0.5°C, Max: 22] for heating (living & kitchen and office) – [Min:17°C, Int:0.5°C, Max:19°C] for heating (bedrooms and short-presence areas e.g., corridors, bathrooms, and WC) -[Min: 23°C, Int: 0.5°C, Max: 25°C] for cooling	[Min: 20°C, Int: 0.5°C, Max: 22] for heating (living & kitchen and office) – [Min:17°C, Int:0.5°C, Max:19°C] for heating (bedrooms and short-presence areas e.g., corridors, bathrooms, and WC) -[Min: 23°C, Int: 0.5°C, Max: 25°C] for cooling
Ventilation rates [m^3/h]	25 m^3/h	25 m^3/h
Fuel type	Natural gas (heating)/ electricity (cooling)	Electricity
Heating	Gas-fired condensing boiler	Air-to-water DX compression
Cooling	Air-to-air DX expansion	Air-to-water DX expansion
Condenser type (cooling)	Air-cooled	Air-cooled
Total cooling capacity [W]	Auto-sized to design days	Auto-sized to design days
Rated EER [−]	[Min: 5.8, Int: 0.5, Max: 8.8]	[Min: 5.4, Int: 0.5, Max: 8.4]
Total heating capacity [W]	Auto-sized to design days	Auto-sized to design days
Rated thermal efficiency/ COP [−]	[Min: 0.88, Int: 0.02, Max: 0.98]	[Min: 4.6, Int: 0.5, Max: 7.6]
Rated Sensible Heat Ratio (SHR)	Auto-sized	–
Coil performance curve type	Bi-Quadratic	Bi-Quadratic
Indoor unit	VAV ADU (cooling)/ water radiator (heating)	Radiant surface heating and cooling (underfloor pipes)
Radiant surface hydronic tubing inside diameter [m]/length [m]/ number of circuits	N/A	0.013 m/auto-sized/one per surface
Rated supply air flow rates (cooling) [m3/s]	Auto-sized	N/A
Design supply air temperature (cooling) [°C]	14°C	N/A
Radiator/radiant surface design capacity [W]	Auto-sized (heating)	Auto-sized (heating and cooling)
Radiator/radiant surface maximum water flow rate [m^3/s]	Auto-sized (heating)	Auto-sized (heating and cooling)
Radiant surface heating/ cooling control throttling range [°C]	N/A	0.5°C
Min/max/design plant loop hot water flow rate [m^3/s]	Auto-sized (variable flow)	Auto-sized (variable flow)
Reference entering hot water temperature [°C]	80°C	35°C
Min/max/design plant loop chilled water flow rate [m^3/s]	N/A	Auto-sized (variable flow)
	N/A	18°C

(continued on next page)

Table 2 (*continued*)

	Gas-fired boiler + air conditioner (S01)	Reversible air-to-water heat Pump (S02)
Design entering chilled water temperature [°C]		
Tank volume [m^3]	N/A	Auto sized
Water tank internal heating element maximum capacity [W]/control type/fuel type/thermal efficiency [−]	N/A	Auto-sized/cycle/ electricity/0.9
Radiant surface condensation control type	N/A	Simple off
AHU type	Variable volume	Constant volume
AHU Fan	Efficiency [Min: 0.70, Int: 0.04, Max: 0.90]/ pressure rise: 600 pa/ motor efficiency: 0.90	Efficiency [Min: 0.70, Int: 0.04, Max: 0.90]/ pressure rise: 600 pa/ motor efficiency: 0.90
AHU design supply flow rate	Auto-sized	Auto-sized
AHU Heat recovery efficiency [−]/heat exchanger type/Frost control type	92%/plate/none	92%/plate/none

Earth System Model (ESM). In addition, Table 3 provides weather summaries per scenario in terms of Heating Degree Days (HDD10°*C*), Cooling Degree Days (CDD18°*C*), average, hottest, and coldest yearly air temperature, and annual cumulative horizontal solar radiation.

According to the weather files used in this paper, the monthly outdoor air temperature is expected to increase between 1.11°*C* to 4.11°*C* in 2090s_SSP5 compared to 2010s. The maximum and minimum changes occur in July and April, respectively. In general, the increases are larger in the summer (July to August) than in the spring (April to June). On an annual basis, there is an increase in air temperature 1.1°*C* by 2050s and 1.6°*C* by 2090s considering the SSP2 scenario, 1.3°*C* by 2050s and 2.6°*C* by 2090s considering the SSP3 scenario, and 1.6°*C* by 2050s and 3.2°*C* by 2090s considering the SSP5 scenario. The *HDD10°C* decreases 24% by 2050s and 42% by 2090s, whereas the *CDD18°C* increases 21% by 2050s and 60% by 2090s averaged over SSPs. The highest hottest temperature 34.7°*C* is resulted for 2090s_SSP3 and the lowest coldest temperature −7.1°*C* is resulted for 2010s. In general, the coldest air temperature during the year increases 3.63°*C* by 2050s and 4.2°*C* by 2090, while the hottest air temperature increases 1.4°*C* by 2050s and 3.7°*C* by 2090s averaged over SSPs. With the increase of *HDD10°C* and the coldest air temperature during the year, it is expected that the average and peak heating loads will decrease in buildings. On the other hand, with the increase of *CDD18°C* and the hottest air temperature during the year, it is expected that the average and peak cooling loads will increase [82–84]. Based on the climate data in this paper, the annual cumulative horizontal solar radiation inconsistently varies between 1024 kWh/m^2 and 1132 kWh/m^2 among different scenarios.

3.2. Time-integrated discomfort

In this section, the result of time-integrated discomfort assessment for the base case building model is described by analyzing the Indoor Overheating Degree (IOhD) and the Indoor Overcooling Degree (IOcD) indices. The *IOhD* and *IOcD* represent the intensity and frequency of

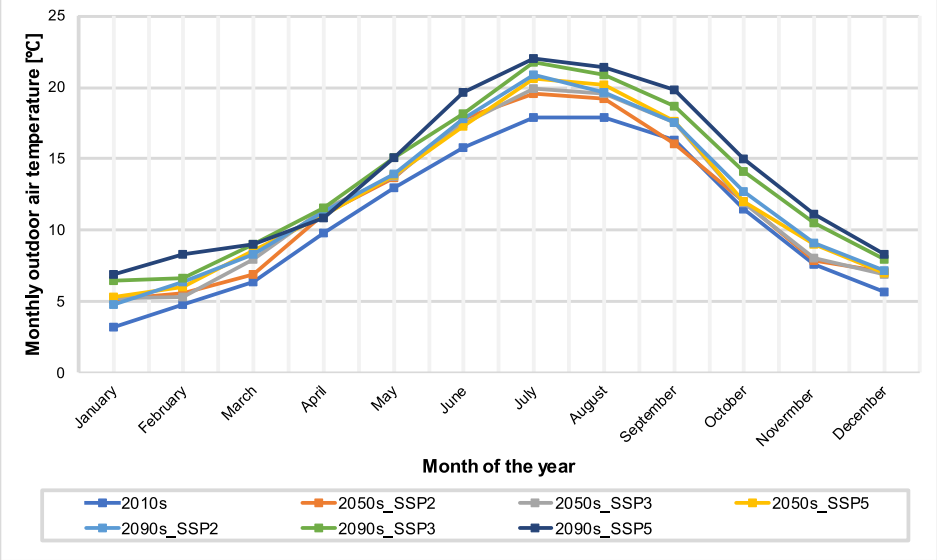

Fig. 4. Monthly outdoor air temperature for current and future TMYs for Brussels resulted from MAR forced by BCC-CSM2-MR Earth System Model (ESM).

Table 3
Summary of weather scenarios in terms of HDD10°*C*, HDD18°*C*, average yearly temperature, hottest temperature (99%), coldest temperature (1%), and annual cumulative horizontal solar radiation.

	HDD10°*C* [Kh]	CDD18°*C* [Kh]	Average yearly temperature [°*C*]	Hottest temperature (99%) [°*C*]	Coldest temperature (1%) [°*C*]	Annual cumulative horizontal solar radiation [**kWh/m²**]
2010s	929	294	10.8	29.8	−7.1	1024.83
2050s_SSP2	738	342	11.9	29.6	−2.3	1111.67
2050s_SSP3	698	343	12.1	31.7	−3.7	1068.57
2050s_SSP5	665	390	12.4	31.9	−4.4	1132.63
2090s_SSP2	672	364	12.4	31.4	−6.9	1092.26
2090s_SSP3	510	488	13.4	34.7	−1.8	1056.92
2090s_SSP5	455	569	14	34.5	0.2	1090.91

overheating and overcooling discomfort considering zonal comfort criteria, respectively. Fig. 5 shows the *IOhD* and *IOcD* for different climate scenarios assuming the static comfort model for the bedrooms and the adaptive comfort model for other zones based on ISO 17772–1 (see Section 2.4).

The *IOhD* increases between 109 and 200% by 2050s and between 154 and 528% by 2090s. On the other hand, the *IOcD* decreases between 11 and 23% by 2050s and between 21 and 32% by 2090s. The overheating discomfort has relatively more variations compared to the overcooling discomfort. It means that the heating system performance (i.e., gas-fired boiler coupled to water radiators) will be less affected by climate change than the cooling system performance (i.e., natural ventilation). It is normal since the effectiveness of natural ventilation is highly dependent on outdoor thermal conditions [85]. Therefore, with the increase in outdoor air temperatures, the cooling effect of natural ventilation will decrease leading to an escalation in the overheating discomfort.

In addition, the results show that the *IOhD* in the current weather scenario (i.e., 2010s) is 85% lower than the *IOcD*. With the continuation of global warming, however, the situation will be reversed. The *IOhD* will become 3.8% and 21% more compared to *IOcD* considering 2090s_SSP3 and 2090s_SSP5, respectively. Therefore, it is predicted in this paper that the overheating discomfort will overlap the overcooling discomfort and will become the major cause of discomfort if the building lacks a proper active cooling system. This is in line with the findings of [12,35,86–88] that the use of active cooling systems along with the passive ones will become inexorable to cope with the overheating impact of climate change in buildings.

The result for the overcooling assessment shows that even though the building is equipped with a heating system, the high values between $0.76°C$ to $0.51°C$ are resulted for *IOcD*. It is since the lower limit of comfort for the static comfort model is $20°C$, whereas the radiators are left half-open by the occupants to meet a set-point temperature of $18°C$ in the bedrooms and short-presence areas [66]. It makes these zones to be accounted as discomfortable during the heating season according to the thermal comfort model. Overall, a low heating set-point temperature can decrease the final heating energy use but forfeits thermal comfort [31].

3.3. Primary energy use and GHG emissions

This section presents the results of the simulations regarding the ranges of heating primary energy use, cooling primary energy use, HVAC primary energy use, and HVAC GHG emissions for S01 and S02. All HVAC components are considered while calculating the HVAC primary energy use and GHG emissions including the heating system, cooling system, and mechanical ventilation. Fig. 6 shows the distribution of the heating primary energy use and the cooling primary energy use for different variations of the input parameters. The point clouds for S01 and S02 are distinguished and colored by the weather scenarios. Moving from the current to future weather scenarios, the points tend towards lower heating primary energy use and higher cooling primary energy use in both S01 and S02.

Fig. 7 depicts the minimum, maximum, median, mean, 25% quartile, 75% quartile, and standard deviation for heating, cooling, and HVAC primary energy use for S01 and S02 under different weather scenarios. To derive the primary energy use, the final energy use is converted using the Primary Energy Factor (PEF) 2.5 for electricity from the grid and 1 for natural gas [89]. The final heating energy use for S01 includes the natural gas consumption of the boiler and electricity consumption of the pump and for S02 includes the electricity consumption of the compressor, the condenser pump, the evaporator fan, and the tank supplementary internal heating coil. The final cooling energy use for S01 includes the electricity consumption of the compressor, the condenser fan, and the evaporator fan and for S02 includes the electricity consumption of the compressor, the evaporator pump, and the condenser fan.

For heating, S01 has ~60% more mean heating primary energy use compared to S02 averaged over all climate scenarios. The mean heating primary energy use for S01 decreases between 19 and 37% from 2010s to 2050s and between 34 and 64% from 2010s to 2090s. While for S02, it decreases between 24 and 38% from 2010s to 2050s and between 32 and 74% from 2010s to 2090s. For cooling, S01 has between 37% and 56% less mean primary energy use than S02. The lowest value is calculated for 2090s_SSP5 and the highest value is calculated for 2010s. It shows that S01 has superior cooling energy performance than S02 in the current climate scenario; however, this superiority will diminish with the increase in outdoor temperatures. The mean cooling primary energy use

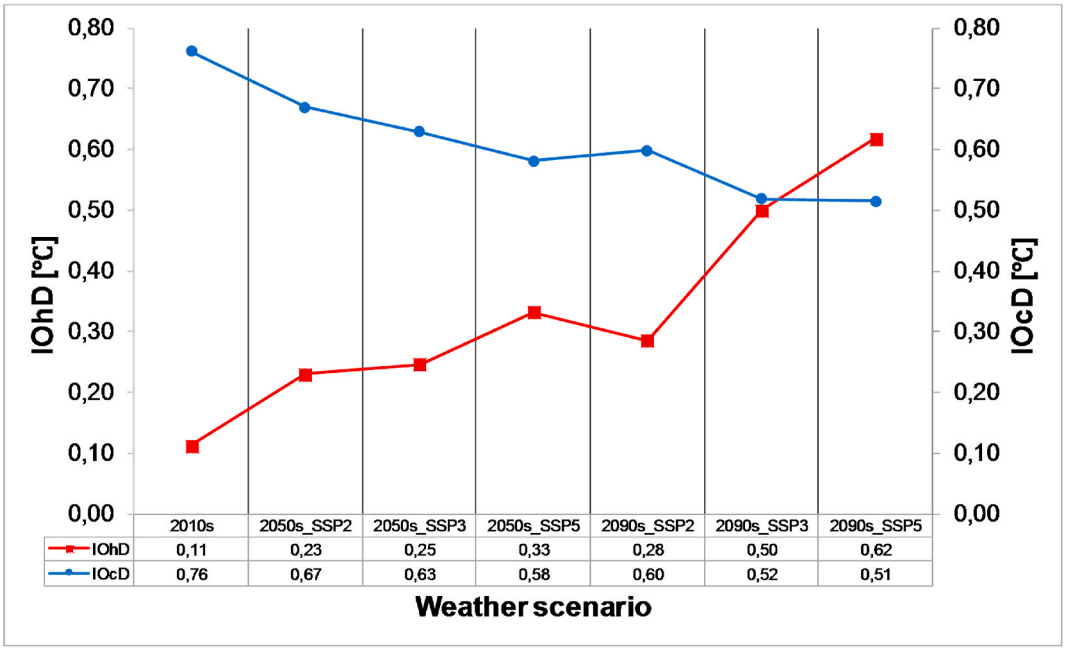

Fig. 5. IOhD and IOcD presented by weather scenario.

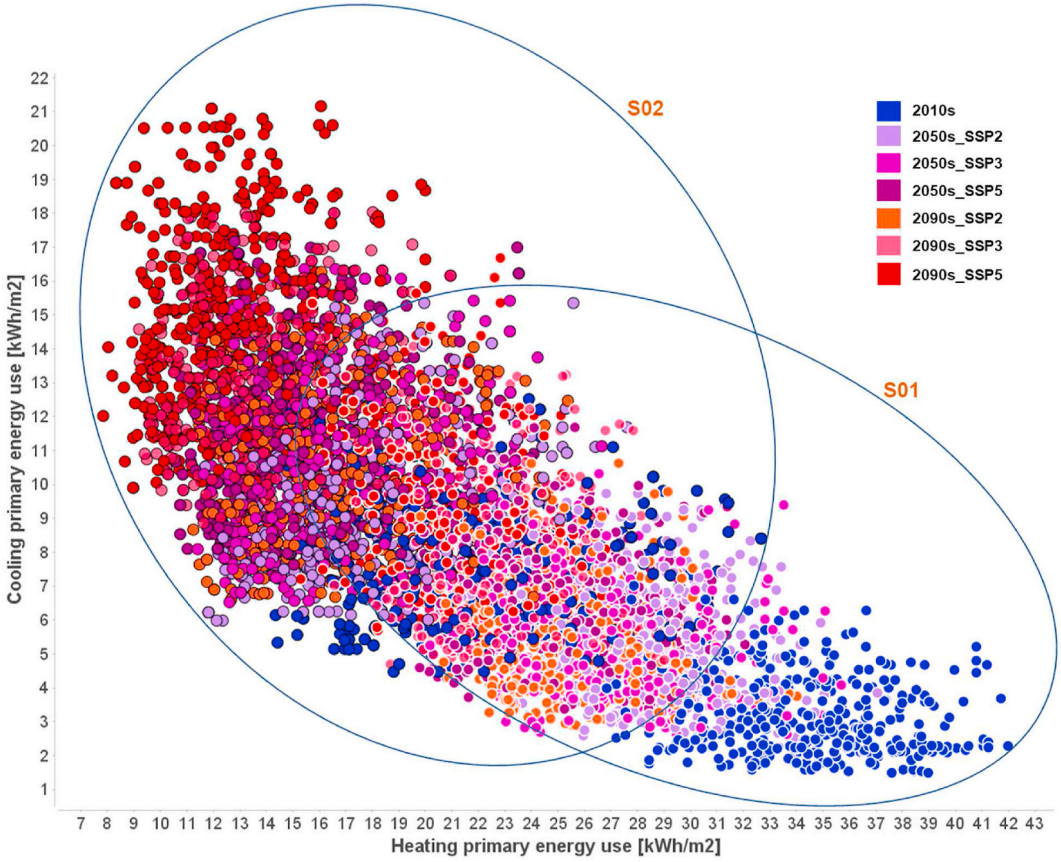

Fig. 6. Scatter plot based on heating and cooling primary energy use colour categorized by weather scenarios for all simulation cases. The point clouds for the case with S01 and S02 are distinguished. (For interpretation of the references to colour in this figure legend, the reader is referred to the Web version of this article.)

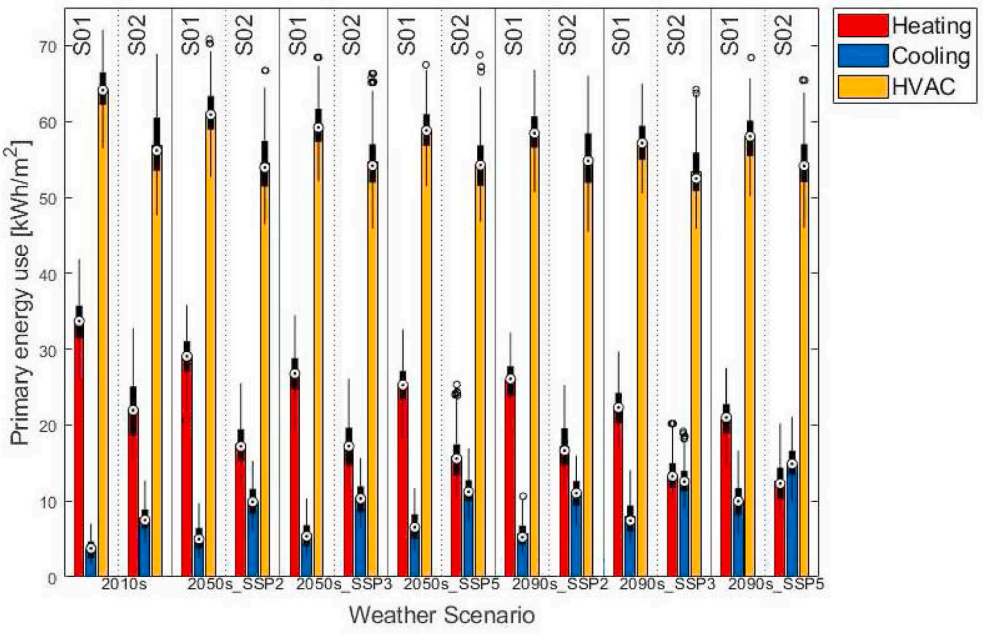

Fig. 7. Bar plots and box plots showing the heating, cooling, and HVAC primary energy use under different weather scenarios.

for S01 increases between 39 and 50% from 2010s to 2050s and between 43 and 65% from 2010s to 2090s. While for S02, it increases between 21 and 33% from 2010s to 2050s and between 28 and 50% from 2010s to 2090s.

The difference between the mean heating and cooling primary energy use for S02 is between 0.73 and 14.06 kWh/m^2. The cooling primary energy use overlaps the heating primary energy use by 2.76 kWh/m^2 in 2090s_SSP5 for S02. It is due to the fact that, a) there is a marginal difference between the *COP* of heating and EER of cooling for the reversible air-to-water heat pump, and b) the *CDD18°C* is 114 Kh more than *HDD10°C* in 2090s_SSP5. For S01, the difference between the mean heating and cooling primary energy use is between 11.07 and 30.66 kWh/m^2 where always the heating primary energy use is more than the cooling primary energy use. Even though the climate-related parameters (i.e., *CDD* and *HDD*) show more need for cooling than heating in 2090s_SSP5, due to the relatively low efficiency of the gas-fired boiler in S01, it remains the major energy consumer in the HVAC system.

Overall, because of lower final heating energy use in S02, the final HVAC energy use is ~29.04 kWh/m^2 less in S02 compared to S01. The difference becomes smaller in terms of the primary energy use due to higher PEF of the electricity than natural gas. S02 has ~4.84 kWh/m^2 less HVAC primary energy use compared to S01. The HVAC primary energy use decreases ~7% for S01 and ~4% for S02 by 2090s compared to 2010s.

The HVAC GHG emissions are calculated using the electricity and natural gas emission intensity derived from the European Environment Agency (EEA) and the report by Joint Research Center (JRC) of the European Commission (EC) [90]. Electricity's GHG intensity is assumed to be 0.161 tCO_2e/MWh and the natural gas's emission intensity is assumed to be 0.240 tCO_2e/MWh. Fig. 8 shows the GHG emissions related to heating, cooling, and ventilation for S01 and S02. It shows a decrease in future GHG emissions that is closely in relation to the warming weather conditions and the decrease in building heating primary energy use. Overall, the HVAC GHG emissions for S02 is lower between 15 and 27% than S01 thanks to lower HVAC primary energy use and lower emission intensity for electricity than natural gas. For S01, the mean HVAC GHG emissions decreases 14%, while for S02, a decrease of 3% is resulted by 2090s. Table B1 in Annex B summarizes the minimum, maximum, median, mean, 25% quartile, 75% quartile, and standards deviation for heating, cooling, and HVAC primary energy use as well as GHG emissions.

3.4. Sensitivity analysis

In this section, the results of Sensitivity Analysis (SA) are presented. Fig. 9 depicts the parallel coordinates showing the interactions between the input and output parameters during the SA process. Fig. 10 plots the Morris SA outcomes considering the HVAC primary energy use as the output parameter. In Fig. 10, the standard deviation of elementary effect (sigma) is an expression of the interaction effect of each input parameter (e.g., *W, T, P0, P1*, …) (i.e., high-order or curvature effects) on the output parameter (i.e., HVAC primary energy use). And, the absolute mean of elementary effect (Mu*) is a measurement of the overall effect of each input parameter (e.g., *W, T, P0, P1,* …) on the output parameter (i.e., HVAC primary energy use) avoiding the cancellation effect [91, 92]. The SA is performed for both S01 and S02 individually and combined (i.e., considering the building model as a discrete input parameter *"M"*).

The findings of this study show that the most influential parameters considering, a) only S01 are cooling set-point *"P7"*, weather scenario *"W"*, and heating set-point for living & kitchen and office *"P5"*, b) only S02 are fan efficiency *"P4"*, heating *COP "P0"*, and cooling set-point *"P7"*, and c) both S01 and S02 are building model (HVAC strategy) *"T"*, heating set-point for living & kitchen and office *"P5"*, and cooling set-point *"P7"*.

Fig. 10 shows that the standard deviation is always strictly positive, therefore none of the influential parameters has a perfectly linear effect on the outcomes. For only S01 case, the largest values of standard deviation (sigma) tend to be associated with the most influential parameters (*"P7" and "W"*). Therefore, *"P7" and "W"* are influential and non-linear/interacting parameters for only S01 case. It means that there is a link between those parameters' amount of influence and their involvement in the curvature effects (i.e., interaction effects). On the other hand, the most influential parameters, *"P4", "P0", and "P7"* for only S02 case and *"T"*, *"P5"*, and *"P7"* for both S01 and S02 case, are not associated with the highest values of sigma. Therefore, those parameters are influential and non-interacting, meaning that while the magnitude of their effect is consistently high for the perturbations in the parameter space, the variation of their elementary effect is quite minor.

The average impact of *"W"* for the combined case (S01 & S02) is low, but the standard deviation is high. This suggests that in particular circumstances (associated with the implementation of S01 system), the weather scenario can have a significant impact on the HVAC primary

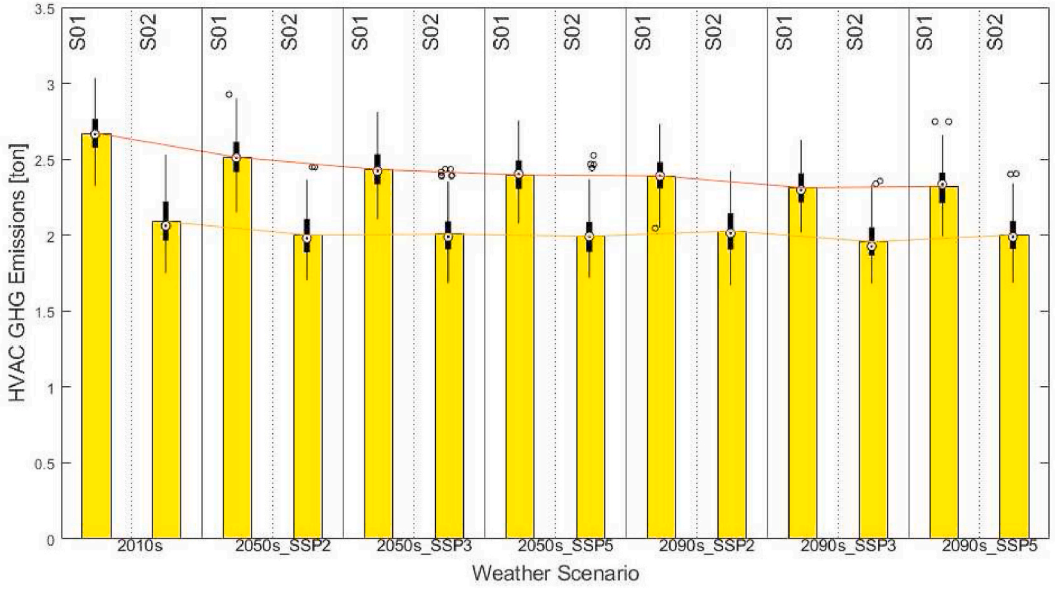

Fig. 8. Bar plots (means) and box plots of GHG emissions by HVAC systems for different weather scenarios.

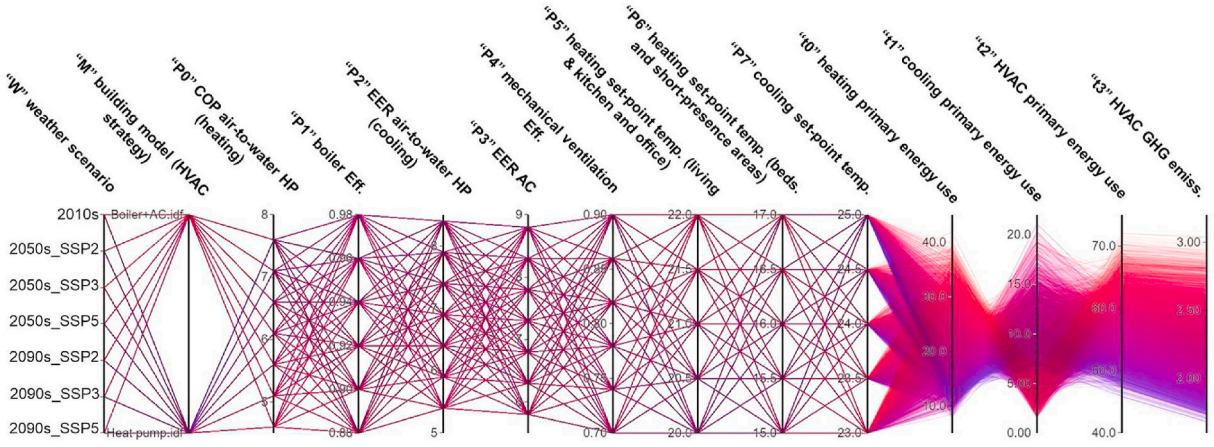

Fig. 9. Parallel coordinates to show the interactions between the input and output parameters in multi-dimensional space of Morris SA (combined case). The lines are colored by HVAC primary energy use.

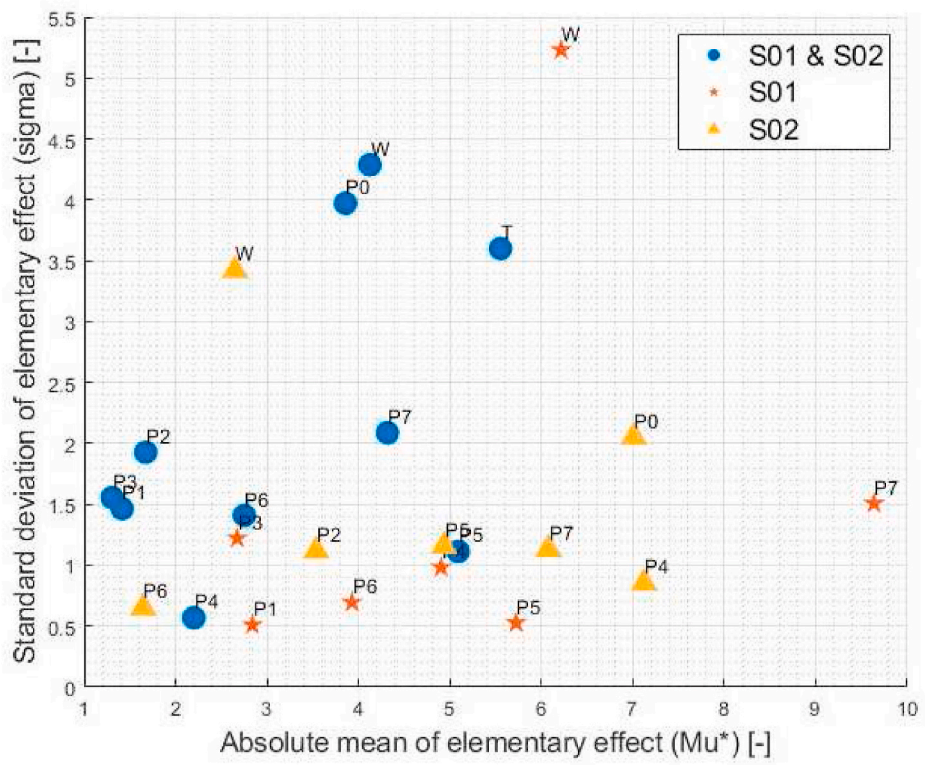

Fig. 10. The Morris sensitivity analysis results, sigma presented by Mu*. The analyses are run for S01 and S02, individually and combined. The output parameter is HVAC primary energy use.

energy use. Table 4 summarizes the input parameters for SA and Morris stats for all cases.

4. Discussion

4.1. Findings and recommendations

According to the Intergovernmental Panel on Climate Change (IPCC), the average global air temperature increased during the past 100 years and will continue to increase due to the release of GHG into the atmosphere. In this paper, the future weather data (MAR BCC-CSM2-MR based on SSP2, SSP3, and SSP5 scenarios) for Brussels city show an increase in the mean annual air temperature $\sim 1.33^{\circ}C$ by 2050s and $\sim 2.46^{\circ}C$ by 2090s. As shown in Fig. 4, with the continuation of global warming, the cooling seasons will be further extended to the shoulder seasons. The winter seasons will become warmer, and the outdoor air temperatures in the range of $\sim 15^{\circ}C$ to $\sim 18^{\circ}C$ will be experienced more. Also, the heatwave events can take place more frequently during the cooling season (i.e., in close occasions) which can make the recovery stage [93] for buildings troublesome. Overall, the future trends of outdoor air temperature show that the cooling energy demand in buildings will increase, in addition to the peak cooling loads, whereas the heating energy demand and peak heating loads will decrease.

The results in Fig. 5 show an increase up to $\sim$324% in overheating discomfort and a decrease up to $\sim$28% in overcooling discomfort by 2090s. It means that climate change is negatively correlated with the comfort of hot summer days and positively correlated with the comfort of cold winter days. In addition, the rise of internal gains due to growing

Table 4
Sensitivity analysis input parameters and Morris stats.

	Parameter	Type	[Discrete values]/[Min., Int., Max.]	Num. of values	Mu			Mu*			Sigma		
					S1	S2	S1 & S2	S1	S2	S1 & S2	S1	S2	S1 & S2
W	Weather data	Disc.	[2010s, 2050s_SSP2, 2050s_SSP3, 2050s_SSP5, 2090s_SSP2, 2090s_SSP3, 2090s_SSP5]	7	−6.13	−2.30	−3.72	6.21	2.65	4.12	5.23	3.42	4.28
T	Building model (HVAC strategy)	Disc.	[Reversible heat pump, gas-fired boiler + AC]	2	–	–	−5.26	–	–	5.55	–	–	3.60
P0	HP heating COP	Disc.	[4.6,0.5,7.6]	7	–	−7.01	−3.85	–	7.01	3.85	–	2.05	3.97
P1	Gas-fired boiler eff.	Disc.	[0.88,0.02,0.98]	6	−2.83	–	−1.41	2.83	–	1.41	0.50	–	1.46
P2	HP cooling EER	Disc.	[5.4,0.5,8.4]	7	–	−3.53	−1.67	–	3.53	1.67	–	1.11	1.92
P3	AC cooling EER	Disc.	[5.8,0.5,8.8]	7	−2.67	–	−1.30	2.67	–	1.30	1.22	–	1.55
P4	Fan eff.	Disc.	[0.7,0.04,0.9]	6	−4.90	−7.12	−1.45	4.90	7.12	2.20	0.98	0.85	0.56
P5	Heating Set point (Living & Kitchen and office)	Disc.	[20,0.5,22]	5	5.72	4.93	5.09	5.72	4.93	5.09	0.52	1.15	1.11
P6	Heating set point (Beds. and short- presence areas)	Disc.	[17,0.5,19]	5	3.92	1.64	2.75	3.92	1.64	2.75	0.69	0.65	1.40
P7	Cooling set point	Disc.	[23,0.5,25]	5	−9.63	−6.07	−4.31	9.63	6.07	4.31	1.50	1.13	2.08

occupancy densities, lifting up comfort expectations, and ageing population growth are reported in previous studies [94–96]. The above will increase the use of active cooling technologies to guarantee favourable and safe indoor thermal environments in the future.

As mentioned earlier, buildings in EU have a major share in energy consumption and GHG emissions. Enhancing building energy efficiency thus plays a critical part in reaching the European Green Deal's ambitious objective of carbon neutrality by 2050. Improvements in building design and systems (e.g., high insulation, efficient electricity-based HVAC systems, etc.) may reduce the direct GHG emissions from the buildings, but it shifts the emissions to the electricity or heating production sector. As shown in Section 3.3, the replacement of a gas-fired boiler + AC with a more efficient reversible heat pump can decrease the final energy use of the building. Whereas, by converting the final energy use to the primary energy use, the difference in the primary energy use between both systems becomes very small (due to the high Primary Energy Factor *"PEF"* for electricity). Therefore, to benefit more from the electrification in buildings in reducing the GHG emissions, it is necessary for the electricity sector to, 1) reduce the losses during the conversion and transformation process (e.g., transmission losses, distribution losses, fuel processing, etc.), and 2) move more towards decarbonized or renewable energy.

According to the results, S02 shows 15–27% lower GHG emissions than S01, considering the current electricity supply conditions (i.e., PEF and energy mix) in Belgium. It shows that the transition from fossil fuel-based (e.g., S01) to more efficient and electricity-based (e.g., S02) HVAC systems can assist a country like Belgium in achieving carbon neutrality and helps in the fight against climate change. It is since, in Belgium, the electricity is generated mostly from renewable energy sources such as wind, solar, and hydro as well as nuclear power [97], implying that future increases in electricity use for heating and cooling will have minimal effects on GHG emissions.

To summarize the significant recommendations, the list below is provided:

- To compensate for the rise of cooling demand in buildings because of climate change, it is recommended to consider highly efficient active cooling systems in combination with passive cooling techniques during the construction of new buildings and the renovation of existing ones.
- In the Belgian context, it is recommended to support electricity-based HVAC systems to enhance the carbon neutrality of buildings. This is valid due to the current energy mix for electricity production in Belgium [97]. The generalizability of the idea to other regions needs further provisions.
- It is recommended to further explore the potential of the reversible air-to-water heat pump coupled with a proper ventilation system as promising heating and cooling strategy in buildings.
- It is also recommended to implement *IOhD* and *IOcD* as principal indicators in time-integrated discomfort evaluations. Designers and decision-makers can use these indicators for a multizonal evaluation of time-integrated discomfort under the operation of different HVAC systems.

4.2. Strengths and limitations

The first strength of the study relies on the validity of the weather data used for the simulations. The weather data in this study are based on the MAR model that has a high spatial resolution (∼5 km), detailed parameterization (takes into account the mesoscale phenomena), and is tuned for the studied region (i.e., Belgium). The study's strength also relates to the selection of a reference building model that represents nearly zero-energy terraced dwellings in Belgium. The simulation model was developed and calibrated in a previous study by some authors of the current paper [66]. This study also compares two commonly applied HVAC strategies in Belgium (gas-fired boiler + AC and reversible air-to-water heat pump) providing detailed information on the system design and sizing. Another strength of the study relates to the application of Uncertainty Analysis (UA) and Sensitivity Analysis (SA). This allows not only to take into account the uncertainties in the HVAC input parameters but also to find the most influential factors affecting the HVAC primary energy use.

However, the study has some limitations. First, in determining time-integrated discomfort, it is also vital to consider relative humidity and other comfort factors such as clothing insulation, metabolic rate, and air velocity. Within the current study's evaluation paradigm, those criteria are ignored. Second, subjective ranges of uncertainty are defined due to the scarcity of data on future predictions of the parameters characterizing the performance of the selected HVAC systems. Third, the degradation of the HVAC systems over time and their replacement with new technologies are neglected. Fourth, the study assesses only three periods (e.g., 2010s, 2050s, and 2090s) based on three SSPs (SSP2, SSP3, and SSP5), disregarding the intermediate periods (e.g., 2030s, 2040s, 2060s, etc.) or other SSP scenarios (e.g., SSP1-1.9 *"very low GHG emissions"* and SSP1-2.6 *"low GHG emissions"*). Therefore, more accurate studies are suggested to overcome the limitations of this paper.

4.3. Implication on practice and future research

Interpreting the outcomes of the current study implies that future revisions of the building codes and regulations must provide provisions regarding the use of active cooling systems. They must include overheating criteria beyond there is a need for the installation of active cooling systems. The overheating compliance must be achieved not only considering the current climate conditions but also for the standardized future climate predictions. The provisions must also incorporate the maximum allowable limits for cooling energy use in addition to the limits for heating energy use. The study enlightens the building designers and professionals regarding the design for climate change. In heating-dominated regions such as Brussels, the focus is mainly to preserve the heat during the winter season to reduce heating energy use, whereas this study shows that overheating and cooling energy use will become dominant in the future. Therefore, together with the comfort and efficiency standards, prudent building design is a key measure to avoid inefficient and uncomfortable units in the coming decades.

This study reveals some future research ideas. First, future research is recommended to perform the same study and compare the results by implementing the weather data obtained from other sources such as CORDEX, Meteonorm, WeatherShift, and CCWorldWeatherGen. Second, it is recommended for future research to analyze the reference buildings representing other building typologies (detached single-family houses, apartment blocks, etc.). Third, future research is encouraged to evaluate other HVAC technologies with more accurate prospective value ranges characterizing their performance. Fourth, future study is needed to enhance the suggested time-integrated discomfort indices (i.e., *IOcD* and *IOhD*). To better reflect the occupant's thermal experience, the new metrics should incorporate more comfort parameters such as relative humidity, metabolic rate, clothing factor, and air velocity.

5. Conclusion

This paper provides a climate change impact assessment for a nearly Zero-Energy dwelling in terms of time-integrated discomfort, HVAC energy performance, and HVAC GHG emissions. In total, seven weather scenarios are used based on regional climate model (MAR) *"Modèle Atmosphérique Régional"* including, the TMYs for 2001–2020 (2010s), 2041–2060 (2050s: SSP2, SSP3, and SSP5), and 2081–2100 (2090s: SSP2, SSP3, and SSP5). In the first stage, a time-integrated discomfort assessment is carried out on the naturally ventilated base case. In the second stage, two commonly applied HVAC strategies including a gas-fired boiler + an air conditioner (AC) (S01) and a reversible air-to-water heat pump (S02) are compared. It is concluded that.

- based on the climate data resulted from MAR forced by BCC-CSM2-MR Earth System Model (ESM), climate change will decrease $HDD10^{\circ}C$ by 42% and increase $CDD18^{\circ}C$ by 60% averaged over three emission scenarios (i.e., SSP2, SSP3, and SSP5) in Brussels by 2090s. Such variations are expected to shift this region from a heating-dominated to a cooling-dominated one.
- with the continuation of global warming, the overheating risk quantified by Indoor Overheating Degree (IOhD) metric will increase between 154 and 528%, whereas the overcooling risk quantified by Indoor Overcooling Degree (IOcD) metric will decrease between 21 and 32% by the end of this century. It is estimated that the overheating risk may overlap the overcooling risk by 2090s under the high emission scenario (i.e., SSP5).
- by 2090s, the HVAC primary energy use decreases ~7% for S01 and ~4% for S02. For S01, the HVAC GHG emissions decrease 14%, while for S02, a decrease of 3% is predicted by 2090s. Overall, the HVAC GHG emissions for S02 is lower between 15 and 27% than S01 thanks to lower heating primary energy use and carbon emission intensity for electricity than natural gas.
- the most influential parameters on the HVAC primary energy use are, a) heating set-point, cooling set-point, and weather scenario for S01, and b) fan efficiency, heating COP, and cooling set-point for S02. The choice of the HVAC system is the most influential parameter while considering it as an input parameter for the sensitivity analysis. Therefore, the selection of the HVAC system during the early-design stages plays a crucial role in determining the energy efficiency in buildings.

Overall, to reach the EU objective of 55% reduction in emissions by 2030 (Fit for 55), it is necessary to advance in four aspects of, a) embracing the end-user electrification in the residential sector, b) improving the efficiency of the building systems, c) reducing the losses during the conversion and transformation process for electricity production, and d) decarbonization of the electricity sector. For this to happen, the current energy renovation rates [98] and replacement of traditional building systems should be accelerated in parallel to increasing the efficiency and share of renewable energy sources in the electricity sector.

CRediT authorship contribution statement

Ramin Rahif: Writing – original draft, Visualization, Validation, Methodology, Investigation, Formal analysis, Data curation, Conceptualization. **Alireza Norouziasas:** Writing – original draft, Visualization, Investigation. **Essam Elnagar:** Writing – review & editing, Validation, Software. **Sébastien Doutreloup:** Writing – review & editing, Validation, Investigation, Formal analysis, Data curation. **Seyed Mohsen Pourkiaei:** Validation, Formal analysis, Data curation. **Deepak Amaripadath:** Writing – original draft, Formal analysis, Data curation, Conceptualization. **Anne-Claude Romain:** Writing – review & editing, Validation, Conceptualization. **Xavier Fettweis:** Writing – review & editing, Validation, Resources, Data curation. **Shady Attia:** Writing – review & editing, Supervision, Resources, Project administration, Funding acquisition, Conceptualization.

Declaration of competing interest

The authors declare that they have no known competing financial interests or personal relationships that could have appeared to influence the work reported in this paper.

Data availability

Data will be made available on request.

Acknowledgments

This research was funded by the Walloon Region under the call 'Actions de Recherche Concertées 2019 (ARC)' (funding number: ARC 19/23-05) and the project OCCuPANt, on the Impacts Of Climate Change on the indoor environmental and energy PerformAnce of buildiNgs in Belgium during summer. The authors would like to gratefully acknowledge the Walloon Region and the University of Liege for funding. We would like to also acknowledge the Sustainable Building Design (SBD) lab at the Faculty of Applied Sciences at the University of Liege for the use of 64-processor workstation during the computation. This study is a part of the International Energy Agency (IEA) EBC Annex 80 – "Resilient cooling of buildings" project activities to define resilient cooling in residential buildings. We also appreciate the guidance and support provided by Mr. Patrick Van Beeck. No potential competing interest was reported by the authors.

Appendix A

Table A.1 summarizes the envelope and operational characteristics of the reference building used for the current study. The building was constructed in the 1930s and renovated after 2010. It was shifted from D to A grade after the renovation according to the Energy Performance Certificate (EPC) rating scheme.

Table A.1
General description of the case study [66].

Description	Value
Number of floors	3
Total area [m^2]	259
Conditioned area [m^2]	173
Unconditioned area [m^2]	86
Number of occupants	4
Total volume [m^3]	873
Window-wall ratio [%]	19
Window U-value [W/m^2K]	1.2
Window G-value [−]	0.6
Solar Heat Gain Coefficient (SHGC) [−]	0.6
Wall surface absorptance [−]	0.9
External wall U-value [W/m^2K]	0.4
Roof U-value [W/m^2K]	0.3
Ground U-value [W/m^2K]	0.3
Attic floor U-value [W/m^2K]	0.8
Airtightness (50 Pa $m^3/h.m^2$) [ACH]	1.58
Occupancy density [m^2/person]	43
Lighting power density [W/m^2]	8–10
Occupancy, lighting, and equipment schedules	Ref. [66]
Holidays	(Easter) start: 30/03 end: 05/04, total: 7 days (Summer) start: 01/08 end: 155/08, total: 15 days (All saint's day) start: 28/10 end: 05/11, total: 7 days (Christmas) start: 24/12 end: 01/01, total: 7 days

Appendix B

Table B.1 summarizes the minimum, maximum, median, mean, 25% quartile, 75% quartile, and standard deviation for heating, cooling, and HVAC primary energy use as well as HVAC GHG emissions.

Table B.1
Minimum, maximum, median, mean, Q1 (25%), Q3 (75%), and standard deviation of heating, cooling, and HVAC primary energy use, and HVAC GHG emissions for the simulation cases.

	No. cases	Min. heating/ cooling/HVAC/ GHG emiss.	Max. heating/ cooling/HVAC/ GHG emiss.	Med. Heating/ cooling/HVAC/ GHG emiss.	Mean heating/ cooling/HVAC/ GHG emiss.	Q1 (25%) heating/ cooling/HVAC/ GHG emiss.	Q3 (75%) heating/ cooling/HVAC/ GHG emiss.	StdDev. heating/ cooling/HVAC/ GHG emiss.
2010s S01	485	26.61/1.49/ 56.43/2.32	41.97/7.01/ 72.04/3.03	33.94/3.05/ 64.09/2.66	33.97/3.31/ 64.22/2.67	31.49/2.28/62.19/ 2.57	36.37/4.23/66.46/ 2.76	3.25/1.20/2.90/ 0.13
2010s S02	493	14.34/4.47/ 47.61/1.74	32.66/12.52/ 68.93/2.53	21.46/7.48/ 56.16/2.06	21.63/7.56/ 56.88/2.08	18.26/6.12/53.49/ 1.96	24.37/8.84/60.49/ 2.22	3.96/1.68/4.50/ 0.16
2050s SSP2 S01	410	20.27/2.53/ 52.69/2.14	37.05/9.73/ 70.81/2.92	28.72/5.28/ 60.89/2.51	28.49/5.51/ 61.07/2.51	26.56/3.93/58.92/ 2.41	30.18/6.80/63.37/ 2.61	2.72/1.77/3.17/ 0.13
2050s SSP2 S02	503	11.69/5.98/ 46.41/1.70	27.60/15.35/ 66.69/2.44	16.86/9.25/ 53.93/1.97	17.38/9.57/ 54.49/2.00	15.05/7.90/51.40/ 1.88	19.31/10.84/ 57.42/2.10	3.17/2.11/3.93/ 0.14
2050s SSP3 S01	411	19.95/2.63/ 52.11/2.10	35.69/10.32/ 68.43/2.81	26.35/5.31/ 59.18/2.42	26.71/5.50/ 59.41/2.43	24.64/4.21/57.28/ 2.33	28.75/6.51/61.67/ 2.53	2.92/1.68/3.15/ 0.13
2050s SSP3 S02	479	11.41/6.52/ 45.88/1.68	26.65/16.35/ 66.30/2.43	15.68/10.48/ 54.16/1.98	16.35/10.59/ 54.65/2.00	13.99/8.83/51.91/ 1.90	18.48/11.93/ 56.98/2.09	2.99/2.21/3.96/ 0.14
2050s SSP5 S01	465	18.26/3.37/ 51.43/2.07	32.05/11.68/ 67.45/2.75	24.56/6.48/ 58.79/2.40	24.71/6.66/ 58.87/2.39	22.36/5.31/56.74/ 2.30	26.81/7.81/60.97/ 2.49	2.99/1.81/3.11/ 0.13
2050s SSP5 S02	482	10.56/7.31/ 46.81/1.71	24.08/17.17/ 68.77/2.52	15.17/11.24/ 54.24/1.99	15.63/11.35/ 54.29/1.99	13.31/9.43/51.49/ 1.89	17.31/12.81/ 56.84/2.08	2.96/2.30/3.74/ 0.13

(*continued on next page*)

Table B.1 (*continued*)

	No. cases	Min. heating/ cooling/HVAC/ GHG emiss.	Max. heating/ cooling/HVAC/ GHG emiss.	Med. Heating/ cooling/HVAC/ GHG emiss.	Mean heating/ cooling/HVAC/ GHG emiss.	Q1 (25%) heating/ cooling/HVAC/ GHG emiss.	Q3 (75%) heating/ cooling/HVAC/ GHG emiss.	StdDev. heating/ cooling/HVAC/ GHG emiss.
2090s SSP2 S01	515	19.55/2.89/ 50.63/2.04	34.02/10.62/ 66.79/2.73	25.00/5.60/ 58.43/2.39	25.24/5.82/ 58.49/2.38	23.32/4.43/56.52/ 2.30	26.90/6.93/60.66/ 2.48	2.61/1.72/2.98/ 0.13
2090s SSP2 S02	481	11.24/6.49/ 45.47/1.66	25.37/16.27/ 66.02/2.42	15.90/10.46/ 54.81/2.01	16.29/10.61/ 55.21/2.02	13.93/8.93/51.88/ 1.90	18.37/12.22/ 58.43/2.14	2.88/2.14/4.14/ 0.15
2090s SSP3 S01	509	15.56/4.54/ 50.51/2.01	29.00/14.36/ 64.98/2.62	21.94/7.76/ 57.13/2.29	22.16/8.04/ 57.28/2.31	20.49/6.41/54.96/ 2.21	23.96/9.52/59.43/ 2.40	2.51/2.14/3.19/ 0.13
2090s SSP3 S02	463	9.19/8.86/45.83/ 1.68	20.94/18.03/ 64.19/2.35	13.28/12.90/ 52.47/1.92	13.78/13.04/ 53.30/1.95	11.64/11.32/ 50.79/1.86	15.83/14.63/ 55.90/2.05	2.67/2.24/3.60/ 0.13
2090s SSP5 S01	433	14.93/5.69/ 50.12/1.99	26.79/16.68/ 68.41/2.74	20.43/9.25/ 58.01/2.33	20.62/9.54/ 57.92/2.32	18.98/7.95/55.45/ 2.21	22.42/10.89/ 50.11/2.41	2.47/2.21/3.35/ 0.14
2090s SSP5 S02	470	7.84/9.90/45.96/ 1.68	19.99/21.16/ 65.47/2.40	12.20/15.16/ 54.15/1.98	12.41/15.17/ 54.53/2.00	10.73/13.02/ 51.97/1.90	13.86/17.29/ 57.01/2.09	2.25/2.71/3.64/ 0.13

▮ Heating, cooling, and HVAC primary energy use: [kWh/m^2], HVAC GHG emissions: [ton].

References

[1] IPCC WGII core writing team, Summary for Policymakers: Climate Change 2022 - Impacts, Adaptation, and Vulnerability, IPCC Geneva, Switzerland, 2022, p. 7 [Online]. Available: https://www.ipcc.ch/report/ar6/wg2/downloads/report/IPCC_AR6_WGII_FinalDraft_FullReport.pdf. (Accessed 21 June 2022).

[2] M. Santamouris, Innovating to zero the building sector in Europe: minimising the energy consumption, eradication of the energy poverty and mitigating the local climate change, Sol. Energy 128 (2016) 61–94, https://doi.org/10.1016/j.solener.2016.01.021.

[3] M. Santamouris, et al., Urban heat island and overheating characteristics in Sydney, Australia. An analysis of multiyear measurements, Sustainability 9 (5) (2017) 712, https://doi.org/10.3390/su9050712.

[4] S.I. Bohnenstengel, S. Evans, P.A. Clark, S.E. Belcher, Simulations of the London urban heat island, Q. J. R. Meteorol. Soc. 137 (659) (Jul. 2011) 1625–1640, https://doi.org/10.1002/qj.855.

[5] T. Oke, The heat island of the urban boundary layer: characteristics, causes and effects, Wind Clim. Cities (1995) 81–107, https://doi.org/10.1007/978-94-017-3686-2_5.

[6] M. Gustin, R.S. McLeod, K.J. Lomas, Forecasting indoor temperatures during heatwaves using time series models, Build. Environ. 143 (Oct. 2018) 727–739, https://doi.org/10.1016/j.buildenv.2018.07.045.

[7] D.P. Jenkins, V. Ingram, S.A. Simpson, S. Patidar, Methods for assessing domestic overheating for future building regulation compliance, Energy Pol. 56 (May 2013) 684–692, https://doi.org/10.1016/j.enpol.2013.01.030.

[8] R. Rahif, M. Hamdy, S. Homaei, C. Zhang, P. Holzer, S. Attia, Simulation-based framework to evaluate resistivity of cooling strategies in buildings against overheating impact of climate change, Build. Environ. (2022), 108599, https://doi.org/10.1016/j.buildenv.2021.108599.

[9] R. Rahif, A. Fani, S. Attia, Climate change sensitive overheating assessment in dwellings: a case study in Belgium, Bruges, Belgium, in: Proceeding of the International Building Simulation Conference, 2021, pp. 30125–30131 [Online]. Available: http://hdl.handle.net/2268/263260.

[10] M. Hamdy, S. Carlucci, P.-J. Hoes, J.L.M. Hensen, The impact of climate change on the overheating risk in dwellings—a Dutch case study, Build. Environ. 122 (Sep. 2017) 307–323, https://doi.org/10.1016/j.buildenv.2017.06.031.

[11] L. Lan, K. Tsuzuki, Y. Liu, Z. Lian, Thermal environment and sleep quality: a review, Energy Build. 149 (2017) 101–113, https://doi.org/10.1016/j.enbuild.2017.05.043Get.

[12] H. Hooyberghs, S. Verbeke, D. Lauwaet, H. Costa, G. Floater, K. De Ridder, Influence of climate change on summer cooling costs and heat stress in urban office buildings, Clim. Change 144 (4) (Oct. 2017) 721–735, https://doi.org/10.1007/s10584-017-2058-1.

[13] B.G. Armstrong, et al., Association of mortality with high temperatures in a temperate climate: England and Wales, J. Epidemiol. Community Health 65 (4) (Apr. 2011), https://doi.org/10.1136/jech.2009.093161. Art. no. 4.

[14] E.M. Kilbourne, Heat waves and hot environments, Public Health Consequences Disasters 245 (1997) 269.

[15] G. Brücker, Vulnerable populations: lessons learnt from the summer 2003 heat waves in Europe, Euro Surveill. 10 (7) (2005) 1–2, https://doi.org/10.2807/esm.10.07.00551-en.

[16] A. Fouillet, et al., Excess mortality related to the August 2003 heat wave in France, Int. Arch. Occup. Environ. Health 80 (1) (2006) 16–24, https://doi.org/10.1007/s00420-006-0089-4.

[17] H. Johnson, S. Kovats, G. McGregor, J. Stedman, M. Gibbs, H. Walton, The impact of the 2003 heat wave on daily mortality in England and Wales and the use of rapid weekly mortality estimates, Euro Surveill. 10 (7) (2005) 15–16, https://doi.org/10.2807/esm.10.07.00558-en.

[18] J. Garssen, C. Harmsen, J. De Beer, The effect of the summer 2003 heat wave on mortality in The Netherlands, Euro Surveill. 10 (7) (2005) 13SP 557–614, https://doi.org/10.2807/esm.10.07.00557-en.

[19] J.-M. Robine, et al., Death toll exceeded 70,000 in Europe during the summer of 2003, C. R. Biol. 331 (2) (Feb. 2008), https://doi.org/10.1016/j.crvi.2007.12.001. Art. no. 2.

[20] Ansi/Ashrae Standard 55, Standard 55–2020: Thermal Environmental Conditions for Human Occupancy, American Society of Heating, Refrigerating and Air Conditioning Engineers, Atlanta, GA, USA, 2020.

[21] R. Rahif, D. Amaripadath, S. Attia, Review on time-integrated overheating evaluation methods for residential buildings in temperate climates of Europe, Energy Build. 252 (Dec. 2021), 111463, https://doi.org/10.1016/j.enbuild.2021.111463.

[22] R.S. McLeod, M. Swainson, Chronic overheating in low carbon urban developments in a temperate climate, Renew. Sustain. Energy Rev. 74 (Jul. 2017) 201–220, https://doi.org/10.1016/j.rser.2016.09.106.

[23] Iso 15927-4, ISO 15927-4: Hygrothermal Performance of Buildings — Calculation and Presentation of Climatic Data — Part 4: Hourly Data for Assessing the Annual Energy Use for Heating and Cooling, 2005. Geneva, Switzerland.

[24] M. Beshir, J.D. Ramsey, Heat stress indices: a review paper, Int. J. Ind. Ergon. 3 (2) (1988) 89–102.

[25] S. Carlucci, L. Pagliano, A review of indices for the long-term evaluation of the general thermal comfort conditions in buildings, Energy Build. 53 (Oct. 2012) 194–205, https://doi.org/10.1016/j.enbuild.2012.06.015.

[26] S. Carlucci, Thermal Comfort Assessment of Buildings, Springer, 2013, https://doi.org/10.1007/978-88-470-5238-3.

[27] Zero Carbon Hub, Impacts of Overheating: Evidence Review, Zero Carbon Hub, London, England, 2015.

[28] European Commission – Department: Energy, Energy Efficiency in Buildings, Brussels, Belgium, 2020 [Online]. Available: https://ec.europa.eu/info/news/focus-energy-efficiency-buildings-2020-lut-17_en. (Accessed 23 June 2022).

[29] G. Martinopoulos, K.T. Papakostas, A.M. Papadopoulos, A comparative review of heating systems in EU countries, based on efficiency and fuel cost, Renew. Sustain. Energy Rev. 90 (Jul. 2018) 687–699, https://doi.org/10.1016/j.rser.2018.03.060.

[30] É. Mata, J. Wanemark, V.M. Nik, A. Sasic Kalagasidis, Economic feasibility of building retrofitting mitigation potentials: climate change uncertainties for Swedish cities, Appl. Energy 242 (May 2019) 1022–1035, https://doi.org/10.1016/j.apenergy.2019.03.042.

[31] P. Jafarpur, U. Berardi, Effects of climate changes on building energy demand and thermal comfort in Canadian office buildings adopting different temperature setpoints, J. Build. Eng. 42 (Oct. 2021), 102725, https://doi.org/10.1016/j.jobe.2021.102725.

[32] T. Wilbanks, et al., Effects of Climate Change on Energy Production and Use in the United States, *US Dep.* Energy Publ., 2008, p. 12.

[33] H. Radhi, Evaluating the potential impact of global warming on the UAE residential buildings – a contribution to reduce the CO2 emissions, Build. Environ. 44 (12) (Dec. 2009) 2451–2462, https://doi.org/10.1016/j.buildenv.2009.04.006.

[34] S.M. Sajjadian, Performance evaluation of well-insulated versions of contemporary wall systems—a case study of London for a warmer climate, Buildings 7 (1) (2017) 6, https://doi.org/10.3390/buildings7010006.

[35] S. Attia, C. Gobin, Climate change effects on Belgian households: a case study of a nearly zero energy building, Energies 13 (20) (2020) 5357, https://doi.org/10.3390/en13205357.

[36] V. Ciancio, F. Salata, S. Falasca, G. Curci, I. Golasi, P. de Wilde, Energy demands of buildings in the framework of climate change: an investigation across Europe,

Sustain. Cities Soc. 60 (Sep. 2020), 102213, https://doi.org/10.1016/j.scs.2020.102213.
[37] A. Machard, C. Inard, J.-M. Alessandrini, C. Pelé, J. Ribéron, A methodology for assembling future weather files including heatwaves for building thermal simulations from the European coordinated regional downscaling experiment (EURO-CORDEX) climate data, Energies 13 (13) (2020) 3424, https://doi.org/10.3390/en13133424.
[38] A. Sabunas, A. Kanapickas, Estimation of climate change impact on energy consumption in a residential building in Kaunas, Lithuania, using HEED Software, 2017 10-12 May 2017, in: Int. Sci. Conf. "Environmental Clim. Technol vol. 128, *CONECT*, Riga Latv, Sep. 2017, pp. 92–99, https://doi.org/10.1016/j.egypro.2017.09.020.
[39] U.Y.A. Tettey, A. Dodoo, L. Gustavsson, Energy use implications of different design strategies for multi-storey residential buildings under future climates, Energy 138 (Nov. 2017) 846–860, https://doi.org/10.1016/j.energy.2017.07.123.
[40] J. Shen, B. Copertaro, L. Sangelantoni, X. Zhang, H. Suo, X. Guan, An early-stage analysis of climate-adaptive designs for multi-family buildings under future climate scenario: case studies in Rome, Italy and Stockholm, Sweden, J. Build. Eng. 27 (Jan. 2020), 100972, https://doi.org/10.1016/j.jobe.2019.100972.
[41] T. Frank, Climate change impacts on building heating and cooling energy demand in Switzerland, Res. Inspires 125 Years EMPA 37 (11) (Nov. 2005) 1175–1185, https://doi.org/10.1016/j.enbuild.2005.06.019.
[42] L. Pajek, J. Potočnik, M. Košir, The effect of a warming climate on the relevance of passive design measures for heating and cooling of European single-family detached buildings, Energy Build. 261 (Apr. 2022), 111947, https://doi.org/10.1016/j.enbuild.2022.111947.
[43] I. Andrić, A. Pina, P. Ferrão, J. Fournier, B. Lacarrière, O. Le Corre, The impact of climate change on building heat demand in different climate types, Energy Build. 149 (Aug. 2017) 225–234, https://doi.org/10.1016/j.enbuild.2017.05.047.
[44] V. Ciancio, et al., Resilience of a building to future climate conditions in three European cities, Energies 12 (23) (2019) 4506.
[45] T. van Hooff, B. Blocken, H.J.P. Timmermans, J.L.M. Hensen, Analysis of the predicted effect of passive climate adaptation measures on energy demand for cooling and heating in a residential building, Energy 94 (Jan. 2016) 811–820, https://doi.org/10.1016/j.energy.2015.11.036.
[46] A. Moazami, V.M. Nik, S. Carlucci, S. Geving, Impacts of future weather data typology on building energy performance – investigating long-term patterns of climate change and extreme weather conditions, Appl. Energy 238 (Mar. 2019) 696–720, https://doi.org/10.1016/j.apenergy.2019.01.085.
[47] V. Pérez-Andreu, C. Aparicio-Fernández, A. Martínez-Ibernón, J.-L. Vivancos, Impact of climate change on heating and cooling energy demand in a residential building in a Mediterranean climate, Energy 165 (Dec. 2018) 63–74, https://doi.org/10.1016/j.energy.2018.09.015.
[48] R.F. De Masi, A. Gigante, S. Ruggiero, G.P. Vanoli, Impact of weather data and climate change projections in the refurbishment design of residential buildings in cooling dominated climate, Appl. Energy 303 (Dec. 2021), 117584, https://doi.org/10.1016/j.apenergy.2021.117584.
[49] Y. Yang, K. Javanroodi, V.M. Nik, Climate change and energy performance of European residential building stocks – a comprehensive impact assessment using climate big data from the coordinated regional climate downscaling experiment, Appl. Energy 298 (Sep. 2021), 117246, https://doi.org/10.1016/j.apenergy.2021.117246.
[50] V.M. Nik, A. Sasic Kalagasidis, Impact study of the climate change on the energy performance of the building stock in Stockholm considering four climate uncertainties, Build. Environ. 60 (Feb. 2013) 291–304, https://doi.org/10.1016/j.buildenv.2012.11.005.
[51] M. Olonscheck, A. Holsten, J.P. Kropp, Heating and cooling energy demand and related emissions of the German residential building stock under climate change, Energy Pol. 39 (9) (Sep. 2011) 4795–4806, https://doi.org/10.1016/j.enpol.2011.06.041.
[52] K. Jylhä, et al., Energy demand for the heating and cooling of residential houses in Finland in a changing climate, Energy Build. 99 (Jul. 2015) 104–116, https://doi.org/10.1016/j.enbuild.2015.04.001.
[53] D. Mauree, E. Naboni, S. Coccolo, A.T.D. Perera, V.M. Nik, J.-L. Scartezzini, A review of assessment methods for the urban environment and its energy sustainability to guarantee climate adaptation of future cities, Renew. Sustain. Energy Rev. 112 (Sep. 2019) 733–746, https://doi.org/10.1016/j.rser.2019.06.005.
[54] M.C. Peel, B.L. Finlayson, T.A. McMahon, Updated world map of the Köppen-Geiger climate classification, Hydrol. Earth Syst. Sci. 11 (5) (Oct. 2007) 1633–1644, https://doi.org/10.5194/hess-11-1633-2007.
[55] Y. Zhang, L. Jankovic, An interactive optimisation engine for building energy performance simulation, United States, in: Presented at the IBPSA Building Simulation Conference, 2017 [Online]. Available: http://www.ibpsa.org/proceedings/BS2017/BS2017_607.pdf.
[56] S. Doutreloup, et al., Historical and future weather data for dynamic building simulations in Belgium using the regional climate model MAR: typical and extreme meteorological year and heatwaves, Earth Syst. Sci. Data 14 (7) (2022) 3039–3051, https://doi.org/10.5194/essd-14-3039-2022.
[57] X. Fettweis, C. Wyard, S. Doutreloup, A. Belleflamme, Noël 2010 en Belgique: neige en Flandre et pluie en Haute-Ardenne, Bull. Société Géographique Liège 68 (2017) 97–107.
[58] C. Wyard, C. Scholzen, S. Doutreloup, É. Hallot, X. Fettweis, Future evolution of the hydroclimatic conditions favouring floods in the south-east of Belgium by 2100 using a regional climate model, Int. J. Climatol. 41 (1) (2021) 647–662, https://doi.org/10.1002/joc.6642.
[59] S. Doutreloup, C. Wyard, C. Amory, C. Kittel, M. Erpicum, X. Fettweis, Sensitivity to convective schemes on precipitation simulated by the regional climate model MAR over Belgium (1987–2017), Atmosphere 10 (1) (2019) 34, https://doi.org/10.3390/atmos10010034.
[60] K. De Ridder, H. Gallée, Land surface–induced regional climate change in southern Israel, J. Appl. Meteorol. 37 (11) (1998) 1470–1485, https://doi.org/10.1175/1520-0450(1998)037<1470:LSIRCC>2.0.CO;2.
[61] H. Hersbach, et al., The ERA5 global reanalysis, Q. J. R. Meteorol. Soc. 146 (730) (2020) 1999–2049, https://doi.org/10.1002/qj.3803.
[62] V. Eyring, et al., Overview of the coupled model Intercomparison project phase 6 (CMIP6) experimental design and organization, Geosci. Model Dev. (GMD) 9 (5) (2016) 1937–1958, https://doi.org/10.5194/gmd-9-1937-2016.
[63] K. Riahi, et al., The Shared Socioeconomic Pathways and their energy, land use, and greenhouse gas emissions implications: an overview, Global Environ. Change 42 (Jan. 2017) 153–168, https://doi.org/10.1016/j.gloenvcha.2016.05.009.
[64] V. Masson-Delmotte, et al., Climate Change 2021: the Physical Science Basis Contribution of Working Group I to the Sixth Assessment Report of the Intergovernmental Panel on Climate Change, 2021.
[65] C. Zhang, et al., IEA EBC Annex 80 - Dynamic Simulation Guideline for the Performance Testing of Resilient Cooling Strategies, Aaalborg University, Dec. 2021 [Online]. Available: https://hdl.handle.net/2268/266179.
[66] S. Attia, T. Canonge, M. Popineau, M. Cuchet, Developing a benchmark model for renovated, nearly zero-energy, terraced dwellings, Appl. Energy 306 (Jan. 2022), 118128, https://doi.org/10.1016/j.apenergy.2021.118128.
[67] S. Attia, Benchmark model for nearly-zero-energy terraced dwellings, Harvard Dataverse, Cambridge, United States, https://dataverse.harvard.edu/dataset.xhtml?persistentId=doi:10.7910/DVN/GJI84W. (Accessed 29 November 2021).
[68] Iso 18523-2, "ISO 18523-2: Energy Performance of Buildings — Schedule and Condition of Building, Zone and Space Usage for Energy Calculation — Part 2: Residential Buildings, 2017. Geneva, Switzerland.
[69] S. Attia, et al., Framework to Evaluate the Resilience of Different Cooling Technologies, IEA Annex 80 – Resilient Cool. Build., 2021, https://doi.org/10.13140/RG.2.2.24588.13447.
[70] A. Cibse Guide, A. Cibse Guide, Environmetnal Design, Chartered Institution of Building Services Engineers, London, UK, 2015, 2015.
[71] Iso 17772-1, ISO 17772-1: Energy performance of Buildings - Indoor Environmental Quality. Part 1: Indoor Environmental Input Parameters for the Design and Assessment of Energy Performance in Buildings", 2017. Geneva, Switzerland.
[72] Ansi/Ashrae Handbook, Handbook–2017: Fundamentals, American Society of Heating, Refrigerating and Air Conditioning Engineers, Atlanta, GA, USA, 2017.
[73] C. Zhang, et al., Resilient cooling strategies – a critical review and qualitative assessment, Energy Build. 251 (Nov. 2021), 111312, https://doi.org/10.1016/j.enbuild.2021.111312.
[74] M. Stein, Large sample properties of simulations using Latin hypercube sampling, Technometrics 29 (2) (1987) 143–151, https://doi.org/10.1080/00401706.1987.10488205.
[75] F. Domínguez-Muñoz, J.M. Cejudo-López, A. Carrillo-Andrés, Uncertainty in peak cooling load calculations, Energy Build. 42 (7) (Jul. 2010) 1010–1018, https://doi.org/10.1016/j.enbuild.2010.01.013.
[76] M.D. McKay, R.J. Beckman, W.J. Conover, A comparison of three methods for selecting values of input variables in the analysis of output from a computer code, Technometrics 42 (1) (2000) 55–61, https://doi.org/10.1080/00401706.2000.10485979.
[77] J.C. Helton, J.D. Johnson, C.J. Sallaberry, C.B. Storlie, Survey of sampling-based methods for uncertainty and sensitivity analysis, Reliab. Eng. Syst. Saf. 91 (10–11) (2006) 1175–1209, https://doi.org/10.1016/j.ress.2005.11.017.
[78] A. Saltelli, S. Tarantola, F. Campolongo, Sensitivity analysis as an ingredient of modeling, Stat. Sci. (2000) 377–395.
[79] M. Balesdent, L. Brevaul, S. Lacaze, S. Missoum, J. Morio, 8 - methods for high-dimensional and computationally intensive models, in: J. Morio, M. Balesdent (Eds.), Estimation of Rare Event Probabilities in Complex Aerospace and Other Systems, Woodhead Publishing, 2016, pp. 109–136, https://doi.org/10.1016/B978-0-08-100091-5.00008-3.
[80] M.D. Morris, Factorial sampling plans for preliminary computational experiments, Technometrics 33 (2) (1991) 161–174, https://doi.org/10.1080/00401706.1991.10484804.
[81] P. Ekström, R. Broed, Sensitivity Analysis Methods and a Biosphere Test Case Implemented in EIKOS, Posiva Working Report 2006-31, 2006. Tech. rep. Posiva Oy, Eurajoki, Finland.
[82] K. Papakostas, N. Kyriakis, Heating and cooling degree-hours for Athens and Thessaloniki, Greece, Renew. Energy 30 (12) (2005) 1873–1880, https://doi.org/10.1016/j.renene.2004.12.002.
[83] D.J. Sailor, Relating residential and commercial sector electricity loads to climate—evaluating state level sensitivities and vulnerabilities, Energy 26 (7) (Jul. 2001) 645–657, https://doi.org/10.1016/S0360-5442(01)00023-8.
[84] A. Ploskić, Q. Wang, Evaluating the potential of reducing peak heating load of a multi-family house using novel heat recovery system, Appl. Therm. Eng. 130 (Feb. 2018) 1182–1190, https://doi.org/10.1016/j.applthermaleng.2017.11.072.
[85] S. Gilani, W. O'Brien, Natural ventilation usability under climate change in Canada and the United States, Build. Res. Inf. 49 (4) (2021) 367–386, https://doi.org/10.1080/09613218.2020.1760775.
[86] H. Wang, Q. Chen, Impact of climate change heating and cooling energy use in buildings in the United States, Energy Build. 82 (Oct. 2014) 428–436, https://doi.org/10.1016/j.enbuild.2014.07.034.

[87] A.D. Peacock, D.P. Jenkins, D. Kane, Investigating the potential of overheating in UK dwellings as a consequence of extant climate change, Large-Scale Wind Power Electr. Mark. Regul. Pap. 38 (7) (Jul. 2010) 3277–3288, https://doi.org/10.1016/j.enpol.2010.01.021.
[88] R. Gupta, M. Gregg, Using UK climate change projections to adapt existing English homes for a warming climate, Build. Environ. 55 (2012) 20–42, https://doi.org/10.1016/j.buildenv.2012.01.014.
[89] IBGE, Performance Energétique des Bâtiments: Guide des exigences et des procédures de la réglementation Travaux PEB en Région de Bruxelles Capitale, 2017. Brussels, Belgium.
[90] B. Koffi, A. Cerutti, M. Duerr, A. Iancu, A. Kona, G. Janssens-Maenhout, CoM Default Emission Factors for the Member States of the European Union, Eur. Comm. Jt. Res. Cent. JRC, 2017.
[91] F. Campolongo, J. Cariboni, A. Saltelli, W. Schoutens, Enhancing the Morris method, in: Proceedings of the 4th International Conference on Sensitivity Analysis of Model Output, 2005, pp. 369–379. Santa Fe, NM.
[92] S. Bertagnolio, Evidence-based Model Calibration for Efficient Building Energy Services, University of Liege, Belgium, 2012 [Online]. Available: http://hdl.handle.net/2268/125650.
[93] S. Attia, et al., Resilient cooling of buildings to protect against heat waves and power outages: key concepts and definition, Energy Build. 239 (May 2021), 110869, https://doi.org/10.1016/j.enbuild.2021.110869.
[94] W. Luan, X. Li, Rapid urbanization and its driving mechanism in the Pan-Third Pole region, Sci. Total Environ. 750 (Jan. 2021), 141270, https://doi.org/10.1016/j.scitotenv.2020.141270.
[95] M. Luo, et al., The dynamics of thermal comfort expectations: the problem, challenge and impication, Build. Environ. 95 (Jan. 2016) 322–329, https://doi.org/10.1016/j.buildenv.2015.07.015.
[96] United Nations, World Population Prospects, 2017 Revision; 2017, U. N. N. Y., 2014.
[97] International Energy Agency (IEA), Data &statistics [Online]. Available: https://www.iea.org/countries/belgium, 2020. (Accessed 28 June 2022).
[98] European Commission, A renovation wave for Europe—greening our buildings, creating jobs, improving lives, Commun. Comm. Eur. Parliam. Counc. Eur. Econ. Soc. Comm. Comm. Reg 662 (2020) 1–26.